CHALMERS
UNIVERSITY OF TECHNOLOGY

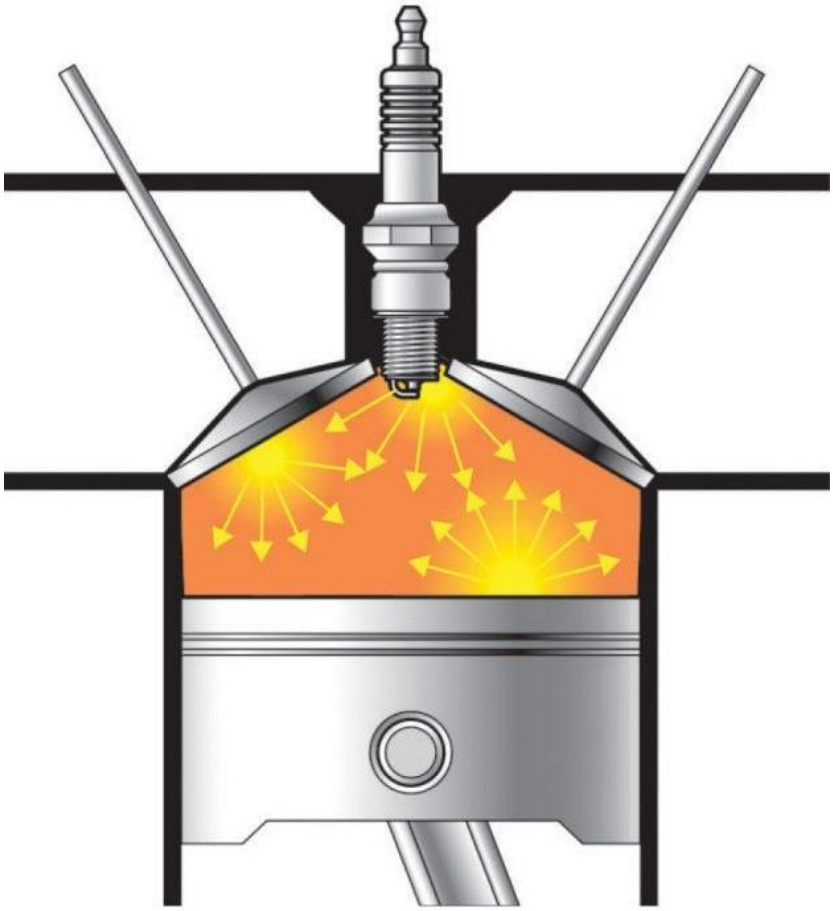

Numerical study of autoignition of fuel-air mixtures at elevated temperatures and pressures

Master's thesis in Automotive Engineering

VINEET TAYUR NAGENDRA & VIKRAM PARAMESHWARA

Department of Mechanics and Maritime Sciences
CHALMERS UNIVERSITY OF TECHNOLOGY
Gothenburg, Sweden 2021

MASTER'S THESIS IN AUTOMOTIVE ENGINEERING

Numerical study of autoignition of fuel-air mixtures at elevated temperatures and pressures

VINEET TAYUR NAGENDRA & VIKRAM PARAMESHWARA

Department of Mechanics and Maritime Sciences
Division of Combustion and Propulsion Systems
CHALMERS UNIVERSITY OF TECHNOLOGY
Göteborg, Sweden 2021

Numerical study of autoignition of fuel-air mixtures at elevated temperatures and pressures

VINEET TAYUR NAGENDRA & VIKRAM PARAMESHWARA

Master's Thesis 2021:06
Department of Mechanics and Maritime Sciences
Division of Combustion and Propulsion Systems

Chalmers University of Technology
SE-412 96 Göteborg
Sweden
Telephone: + 46 (0)31-772 1000

Cover:
A typical case for autoignition of the air-fuel mixture leading to irregular combustion called knocking. Courtesy of the website – 'carfromjapan.com'

Printed by Department of Mechanics and Maritime Sciences / Chalmers University of Technology
Göteborg, Sweden 2021-03-01

Abstract

In a conventional spark-ignition (SI) engine the fuel-air mixture is injected into the cylinder where it is mixed with the residual gasses and compressed. Under normal operation, combustion takes place at the end of the compression stroke, the mixture is ignited by a spark, flame kernel grows, turbulent flame develops and propagates to the walls where it is quenched. As we strive for better thermal efficiency, the compression ratio is the ideal parameter to increase. However, a phenomenon called knock occurs at elevated temperatures and pressures and impedes the improvements to thermal efficiency by simply increasing the compression ratio. Knock occurs because of auto-ignition initiated locally in hot spots in the unburnt fuel-air mixture ahead of the advancing flame front. It deteriorates the working characteristics of the engine and drastically reduces its durability.

Previously, most of the research into knock was carried out experimentally. The recent developments in computer hardware, software, and dedicated chemical kinetic mechanisms that can accurately model the behaviour of gasoline have made it possible to calculate the autoignition of fuels with acceptable accuracy. The main objective of this project is to study the autoignition behaviour of various fuel-air mixtures at elevated temperatures and pressures using the aforementioned chemical kinetic mechanisms.

The autoignition of commercially available fuels is the focus of this thesis. The chemical kinetic mechanisms chosen are from RWTH Aachen University, King Abdullah University of Science, and Technology and Lawrence Livermore National Laboratory. Using the software CHEMKIN-Pro, these mechanisms are adopted to simulate the ignition delay times of iso-octane, n-heptane, and primary reference fuel blended with ethanol (PRF-E) at various temperatures, pressures, and equivalence ratios (fuel-air ratio). The calculated values of ignition delay times are compared with the experimental data available for the same input parameters and the chemical mechanisms from Aachen university is chosen based on the accuracy of the results and the speed of computations.

Using the selected mechanism, ignition delay times for E10 (fuel of RON95 with 10% ethanol by volume), 95 unleaded (RON95), and 98 unleaded (RON98) are calculated. The knock prediction model by Kalghatgi et al., 2017 is used as the criterion for suggesting the best operating range temperature range of the fuels to avoid knock in an engine. Using MATLAB and Excel, graphs for the calculated ignition delay times vs temperature are plotted to study the dependence of various input parameters (temperature, pressure, equivalence ratio, and fuel composition).

The following results are observed:

- The ignition delay times reduce with an increase in the input pressure at a particular temperature.
- The ignition delay times decrease with an increase in equivalence ratio (ϕ).
- The knock resistance of a fuel increases with an increase in the RON of a fuel.
- The ignition delay times reduce with an increase in temperature at a particular pressure.

Keywords: Knock, Auto-ignition, Ignition delay.

Contents

Acknowledgments

We would like to thank our supervisor Andrei Lipatnikov for his help, guidance, and for providing us the opportunity to work on this thesis. We would like to thank our examiner Sven B. Andersson for his input and support. We would also like to thank the department of mechanics and maritime sciences for their warm welcome.

Finally, a heartfelt thank you to our friends and families who have encouraged and helped us in the hard times during this thesis.

Göteborg, March 2021

VINEET TAYUR NAGENDRA & VIKRAM PARAMESHWARA

1 Introduction

Even with the increasing interest in electric vehicles and alternative biofuels, petroleum fuels are still the preferred transport sector choice. Environmental awareness has increased considerably, and stringent regulations have been imposed on CO2 emissions. The way to have cleaner emissions and higher fuel saving is by increasing the efficiency of an engine's ability to convert the chemical energy from the fuel to power. The biggest hurdle in increasing the thermal efficiency of a spark-ignition (SI) engine is the phenomenon called "knock", which increases with the increase in the compression ratio. The name knock is derived by the engine's noise when a portion of the fuel-air mixture auto-ignites. Knocking can have detrimental effects on the engine and should be avoided.

In recent years, computational fluid dynamics (CFD) simulations are often used to study the combustion process, and accurate reaction paths form the foundation for these simulations. Research into gasoline fuels has shown that its behaviour can be reproduced by simple fuel surrogates containing few key components and reactions. For gasoline fuel, generally used in spark-ignition engines, the Primary Reference Fuel (PRF) mixture of n-heptane and iso-octane is often suggested as the surrogate mixture. A kinetic mechanism for these mixtures should be able to show the high-fidelity modelling of a single component effectively and should also be able to imitate the combustion properties of a PRF mixture accurately.

In this chapter, the summary of existing knowledge (Textbooks by John B. Heywood: Internal Combustion Engine fundamentals [1] and Richard Stone: Introduction to Internal combustion Engines [2]) and former performed research about combustion, knocking, and autoignition theory used for knock prediction is presented ([3] - [8]).

The cause of knock over the full range of the engine conditions is still not completely understood. The non-uniform nature of this sudden increase in pressure causes shock waves to propagate in the engine chamber, which causes the chamber to resonate at its natural frequency, which can be harmful to the engine. The autoignition theory has been postulated to explain the cause of knock. It states that when the fuel-air mixture in the end-gas ahead of the flame is compressed to sufficiently high pressures and temperatures, the air-fuel mixture spontaneously combusts in certain hot spots in the end-gas. This theory has attempted to give us a relatively realistic theory as to what causes the rapid release of energy in the end-gas, which creates very high pressures, locally, in the end-gas region [1].

This thesis aims to calculate the ignition delay times for a wide range of temperatures and pressures to study the autoignition behaviour with respect to various input parameters and to suggest the best operating range of different fuel blends to avoid knock. Ignition delay times are calculated using advanced computational tools (Chemkin-Pro) and chemical mechanisms.

1.1 Knocking as a physical phenomenon

To understand knocking as a physical phenomenon, the combustion process is discussed below. The combustion process: mixing of air and fuel in the intake system, injection of the fuel-air mixture (including exhaust gas in an EGR system) into the

cylinder and mixing with residual gases from the previous cycle, ignition of the charge from an electric discharge (power generation) and finally exhaust gases exit the cylinder. The power generation cycle (combustion cycle) is explained further from the time of the spark ignition to the flame quenching:

- Spark ignition: After the air-fuel mixture is injected into the cylinder, a spark from the spark plug leads to the start of the combustion process in the chamber. This usually happens in the compression stroke of the engine, which usually happens between -30° and 0° Crank Angle Degrees (CAD), depending on the load condition on the engine. This spark initiates the combustion process of the air-fuel mixture and the reactions from this combustion results in the formations of radicals.

- Flame development: When the formation of radicals from the combustion process crosses a critical limit, multiple chain reactions occur which results in the formation of more radicals at a faster rate. This results in the flame formation and consumption of the air-fuel mixture.

- Flame propagation: The increase in the radical formation rate leads to an increase in the consumption of the aif-fuel mixture. This causes the flame to propagate further away from the region of spark-ignition. The flame propagation depends on factors like the reactant composition, Exhaust Gas Recirculation (EGR), turbulence, etc. The air-fuel mixture ahead of the flame (which is yet to be consumed) is called end-gas.

- Flame quenching: The flame propagates and when it reaches the walls of the cylinder, the complete air-fuel mixture is consumed (normal combustion circumstances), and the flame dies out.

In an SI engine, abnormal combustion phenomenon can occur in numerous ways, but in this thesis work, the abnormal phenomenon of knocking is explored, which, as explained, leads to catastrophic engine damage or failure. Knocking may occur due to two reasons: auto-ignition in localized hot spots in the unburned charge and surface ignition. Autoignition is the term used for spontaneous and rapid combustion reaction of the end-gas mixture, which is not initiated by the spark ignition [1]. This spontaneous combustion is what causes the ‘knock’. The auto-ignition in the unburned charge creates an alternate flame front, which then collides with the normal flame front causing high-intensity pressure oscillations in the engine. Surface ignition occurs in the hot spots on the chamber walls (due to the previous combustion cycle), hot spark plug, or hot valves. Surface ignition is further classified into pre-ignition or post ignition. As the names suggest, they are the autoignition of the charge before or after the spark discharge. Knock occurrence also depends on various parameters like pressure and temperature of the end-gas, spark advance or retardation, combustion phasing, turbulence in the cylinder, etc.

1.2 Knock resistance

The autoignition of a fuel varies with its composition and some fuels have higher autoignition temperatures than the others and to understand this resistance to knock in SI engines, the research octane number (RON) and motor octane number (MON)

were adopted. RON is used to study the fuel at low temperatures and low speeds and MON at high temperatures and high speeds. There are standardized test methods set by the American Society for Testing and Materials (ASTM) to find the RON (ASTM – D2699) [4] and MON (ASTM – D2700) [5] of various fuels and fuel blends. An increase in octane number leads to increase in resistance to knock (autoignition). During the tests, different compositions of the primary reference fuel (PRF) are tested by varying the iso-octane and n-heptane composition to the point where knock is observed. Most non-PRF fuels have a higher RON compared to their MON. While RON and MON have an important role in the knock resistance of PRF fuels, they are not sufficient to describe the knock resistance of all fuels. Khalgatgi et al. [6] proposed the octane index (OI), which is defined as:

$$OI = K \cdot MON + (1 - K) \cdot RON \quad (1)$$

The constant K depends on pressure and temperature and S (difference between RON and MON) is known as the sensitivity of the fuel. So, by this, one can understand the behavior of a fuel using its RON and MON at specific temperatures and pressures regardless of the engine conditions.

K tends to be negative in the knock-limited regions in SI engines [6]. In recent times, advancement in engine design, like advanced cooling systems, boost system, and injection systems, have contributed to the decrease of K. As the RON and MON tests were defined in the 1920s, the operating conditions of engines today tends to exceed the boundary defined by RON and MON tests.

2 Background

2.1 Fundamentals

2.1.1 Autoignition of Hydrogen-Oxygen system

The autoignition of the hydrogen-oxygen system will be discussed in this section from Ref. [1]. Autoignition is the term used for spontaneous and rapid combustion reactions of the end-gas mixture, which is not initiated by the spark ignition. This spontaneous combustion is what causes the knock. The process will be explained with the autoignition behaviour of a much simpler hydrogen-oxygen system. The chemical reactions which cause the fuel molecules to be broken down and release energy and to form the by-products of combustion in petroleum fuels are extremely complicated and not yet understood in depth.

The autoignition of a fuel-air mixture is mainly controlled by the competition between branching and inhibition reactions. When the energy released by the combustion of the air-fuel mixture is greater than the engine's ability to dissipate the heat from the engine walls, the temperature of the mixture increases, which accelerates the rate of the chemical reactions in the engine leading to spontaneous ignition [1].

In complex reacting systems such as combustion, the reaction consists of a large number of simultaneous and interdependent chain reactions. There is an initiating reaction in such chains where highly reactive intermediate species or radicals are produced from stable molecules (fuel-air mixture). The next step is flame propagation where these radicals start to react with the other molecules in the air-fuel mixture to form end products and other radicals, and these radicals again continue the chain. Some of these reactions produce two radical molecules for each radical consumed and are termed chain-branching reactions. As the rate of formation of the radicals from chain-branching increases rapidly, it results in a 'chain-branching explosion' [1].

The oxidation of hydrogen at high pressures and temperatures provides a good understanding of these phenomena. For the stoichiometric hydrogen-oxygen mixture, no reaction occurs below 400°C unless the mixture is ignited by an external source such as a spark; above 600°C, an explosion occurs spontaneously at all pressures [1].

The initiating steps proceed primarily through hydrogen peroxide (H2O2) to form the hydroxyl radical (OH) at lower temperatures or dissociate H2 at higher temperatures to form the hydrogen atom radical H. The basic radical-producing chain reaction is composed of the following reactions:

R 1 $H + O_2 = O + OH$

R 2 $O + H_2 = H + OH$

R 3 $H_2 + OH = H_2O + H$

The first two reactions are chain-branching; two radicals are produced for every radical consumed. The third reaction is necessary to complete the chain sequence: starting with one hydrogen atom, the sequence R1, then R2 and R3 produce two H; starting with OH, the reactions R3, then R1, then R2 produces two OH. Since all three reactions are required, the multiplication factor is less than 2 but greater than 1. This

sequence of reactions rapidly builds up high concentrations of radicals from low initial levels.

However, these three reactions do not correspond to the overall stoichiometry.

R 4 $H_2 + ½O_2 = H_2O$

A quasi equilibrium is established; while the overall process has proceeded a considerable way toward completion, a substantial amount of the available energy is still contained in the high radical concentrations. Over a longer timescale, this energy is released though three-body recombination reactions:

R 5 $H + H + M = H_2 + M$

R 6 $O + O + M = O_2 + M$

R 7 $H + OH + M = H_2O + M$

M refers to any available third-body species required in these recombination reactions to remove the excess energy.

With this understanding of autoignition in the hydrogen-oxygen system, we can now try to understand the behaviour of the autoignition of hydrocarbon-air mixtures. The process or reaction by which a hydrocarbon in the fuel-air mixture is oxidized can exhibit four different types of behaviour. It can also be a sequential combination of all four bevaiours, depending on the pressure and temperature of the mixture: slow reactions; single or multiple cool flames (slightly exothermic reactions); two-stage ignition (cool flame followed by a hot flame); single-stage ignition (hot flame). Slow reactions are a low-pressure, low-temperature (<200°C) phenomenon which does not normally occur in engines. At 300°C to 400°C, one or more combustion waves often appear, accompanied by blue light emission, which is known as a cool flame. This is because the reaction stops when only a small portion of the reactants have reacted, and the temperature rise is very low. Depending on the engine conditions and the fuel composition, this cool flame may, sometimes, be followed by a "hot flame" or high-temperature explosion where there is a sudden acceleration in the reaction rate after ignition. This cool flame, followed by a hot flame, is known as a two-stage ignition. At higher temperatures, only the single-stage ignition is observed. Some hydrocarbon compounds, however, do not exhibit this cool flame or two-stage ignition behaviour [1].

2.1.2 Negative Temperature Coefficient (NTC)

An important behaviour of large hydrocarbons is the NTC. Figure 1. shows the ignition delay times calculated for a stoichiometric mixture of n-heptane/air at 13.5bar pressure [10]. The curve shows the typical S-shape caused due to NTC behaviour. As explained in the previous section, most hydrocarbons exhibit a two-stage ignition where a cool flame (at low temperatures) is followed by a hot flame (at high temperatures). Normally, an increase in the initial temperature leads to shorter ignition delay times. However, in the temperature region of 800K – 950K, an increase in the initial temperature leads to an increase in the ignition delay times for low initial temperatures. This temperature range is known as the NTC region. As we move

towards the high temperature region, the NTC behaviour is not seen due to the single-stage ignition (hot-flame). The NTC behaviour is very important in understand the low-temperature ignition behaviour of hydrocarbons as these involve cool flames in engine knock, fuel reforming [11] and accidental explosions.

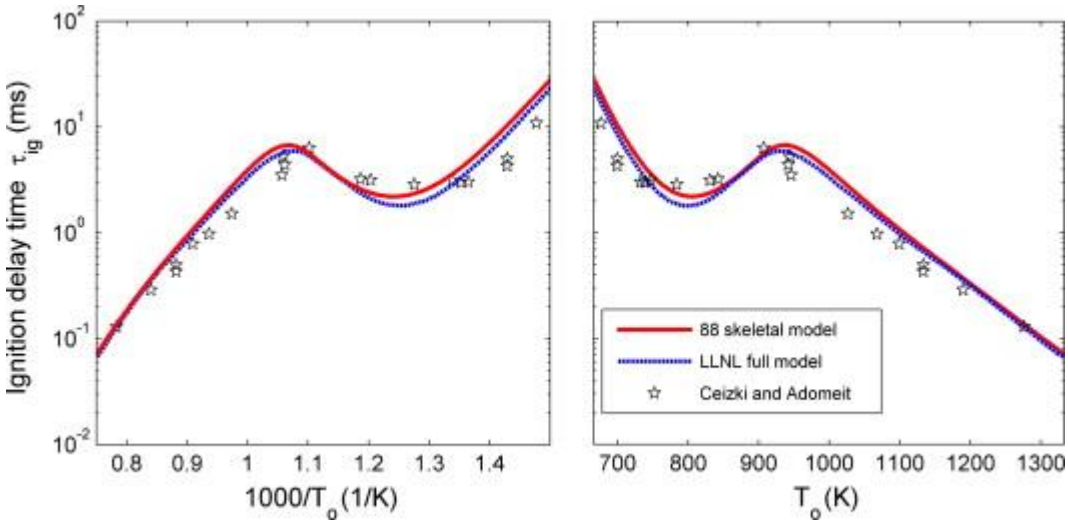

Figure 1: Comparison of calculated ignition delay by Law, C. K, et al, of n-heptane/air mixture of unity equivalence ratio and 13.5 bar pressure with shock tube experimental result of Ciezki and Adomeit [10] (from Ref [12]).

2.1.3 Livengood-Wu Integral

The Chemical kinetic models which are discussed in this thesis are extremely useful in the design stage of an engine. However, the processing power required to run complex simulations according to engine conditions is very high. It is necessary to use simpler models that can show the general characteristics of the engine and in this context, Livengood and Wu [13] proposed a correlation that enables us to calculate the autoignition delay period under engine conditions using the ignition characteristics at constant volume. The correlation is given by the formula:

$$I = \int_{t_0}^{t_i} \frac{dt}{\tau(P,T)} = 1 \qquad 2$$

In the above correlation, t_i is the ignition delay period under engine conditions, τ is the instantaneous ignition delay at pressure (P) and temperature (T) conditions pertaining to time (t), and t_0 is the initial time used for calculations (beginning of compression stroke).

This integration method assumes that the oxidation of a fuel can be described by a single global reaction and that autoignition takes place when a critical concentration of the products of this reaction (xc) is reached. These authors also presume that the ignition delay measures the reaction rate of the global reaction before combustion, and thus, there is a functional relationship between the concentration ratio (x/xc) and the relative time (t/t). Further consideration that the value xc is independent of the initial conditions and that the reaction rate of the global reaction does not depend on time during a constant volume evolution leads to equation (2).

2.2 Methods of research

Due to the above discussed adverse effects of knocking on the engine, it has been one of the most important areas of research over the years. Knock prediction studies have been predominantly studied using the below models:

1. *Empirical Correlation Models (ECMs)*: As the name suggests, these models are used to predict knock using empirical data obtained experimentally. These models can be used to predict knock in any engine regardless of the engine geometry or any other physical parameter. The downside of this model is the lower accuracy due to various assumptions. However, this model can be used along with chemical kinetic models to provide better accuracy than using purely mathematical input. Some models also consider the thermodynamic parameters in the engine during combustion.

2. *Chemical Kinetics Models (CKMs)*: Combustion in an engine is the oxidization of the fuel. Chemical kinetic models are comprised of detailed chemical reactions that take place during this oxidization process. These models use the basics of chemical kinetics to calculate the possibility of knock in the fuel. CKMs can calculate the concentration of the reactants, mass fractions of the species, etc. The autoignition of the fuel can be studied by varying the input parameters to the combustion process and without any engine parameters.

3. *Computational Fluid Dynamics Models (CFDMs)*: These models require the estimation of the physical parameters of the end-gas in the engine to accurately simulate the combustion process. The engine geometry is crucial for these models. Since these models depend on the engine geometry, each point in the piston movement requires a separate simulation.

2.3 Dependency of Ignition delay on various parameters

2.3.1 Fuel Chemistry and Knock resistance

When the pressure of the system is 15bar, the volume is known. The number of moles of air, fuel, and an estimate of the residual gas are known. The temperature (T) at this pressure of 15bar is calculated from the universal gas equation:

$$PV = mRT \qquad 3$$

P: pressure, V: volume, m: number of moles of the gas, R: universal gas constant and T: temperature. This is T_{comp15} [14] - [19].

To use equation 2, the term T_{comp15} was introduced by Kalghatgi, and K was expressed as a function of this temperature.

The correlation for K with unburnt gas temperature (T_{comp15}) was plotted by Boot et al. [20] As shown in Figure 2., K values tend to be negative as T_{comp15} goes lower than the corresponding temperature for the RON test. T_{comp15} is lower in modern SI engines due to the lower intake pressure as compared to the RON and MON tests.

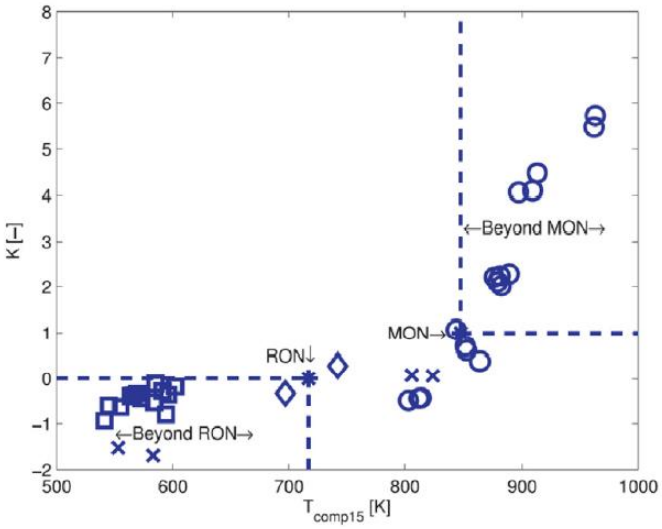

Figure 2: K versus Tcomp15 (from Ref. [3]).

While the above fuel indices (RON, MON, and OI) have been used to describe anti-knock properties, their relationship is not clear and the reason for this being the autoignition in engines is directly related to the combustion chemistry of hydrocarbons at different operating conditions.

The ignition delay times are used to investigate the reactivity in terms of auto-ignition propensity at different operating conditions. The Octane sensitivity of a fuel tells us the dependence of chemical reactivity of the fuel with temperature and pressure. Also, the slope of the ignition curve in the NTC regime (S-shaped curve) is another indicator of the reactivity of the fuel.

2.3.2 Effect of pressure on Ignition delay times

Mohammed AlAbbad et al. [8] performed ignition delay time measurements for PRF fuel blends at pressures of 10, 20, and 40bar using the Mehl et al. Mechanism [21]. Figure 3. shows the effect of pressure on a fuel of PRF 70 and for ϕ = 0.5, 1 (ϕ is the equivalence ratio or the fuel-air ratio. ϕ<1 is a lean mixture, ϕ=1 is a stoichiometric mixture and ϕ>1 is a rich mixture) and PRF 91 for ϕ = 1. In Figure3. we can observe that increase in pressure leads to shorter ignition delay times of the PRF blends. The NTC region shows the highest variation with pressure. As the pressure increases, the NTC region is seen to flatten out and is less pronounced. In Ref. [8], the authors attributed the less pronounced NTC at higher pressures to the increased stability of the RO_2 radical and higher decomposition rate of H_2O_2. The authors also observed that Stoichiometric mixtures showed a higher pressure dependency as compared to lean mixtures.

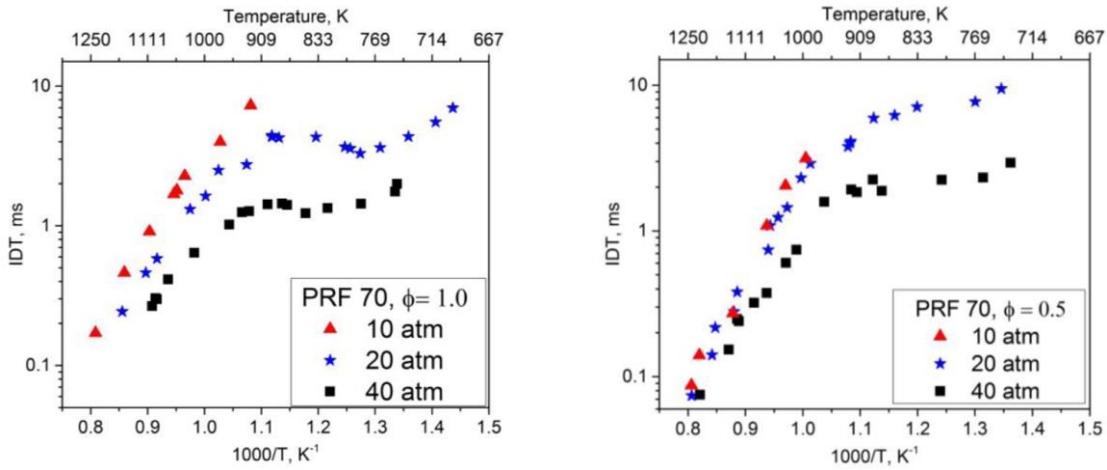

Figure 3: Influence of pressure on ignition delay times calculated using the Mehl et al. Mechanism[22]. (a) PRF 70 (ϕ = 1), (b) PRF 70 (ϕ = 0.5) (from Ref. [8]).

2.3.3 Effect of equivalence ratio (ϕ) on ignition delay times

Mohammed AlAbbad et al. [8] measured the ignition delay times for all PRF blends at lean (ϕ = 0.5) and stoichiometric conditions (ϕ = 1). Figure 4. shows the effect of equivalence ratio on ignition delay times for a fuel of PRF 70 and at a pressure of 40bar. The authors observed that the ignition delay times decrease with an increase in ϕ and the effect of ϕ was highest in the NTC region. In the high- and low-temperature regions, ignition delay times exhibited weak dependence on ϕ. By conducting a sensitivity analysis for PRF 70 at 800K and 40bar pressure (ϕ=0.5,1), the authors attributed the high dependency in the NTC region to the hydroperoxyl radical chemistry. At lean conditions, they observed that the reaction of hydrogen peroxide with oxygen played a strong inhibiting role and hence smaller reactivity for lean mixtures.

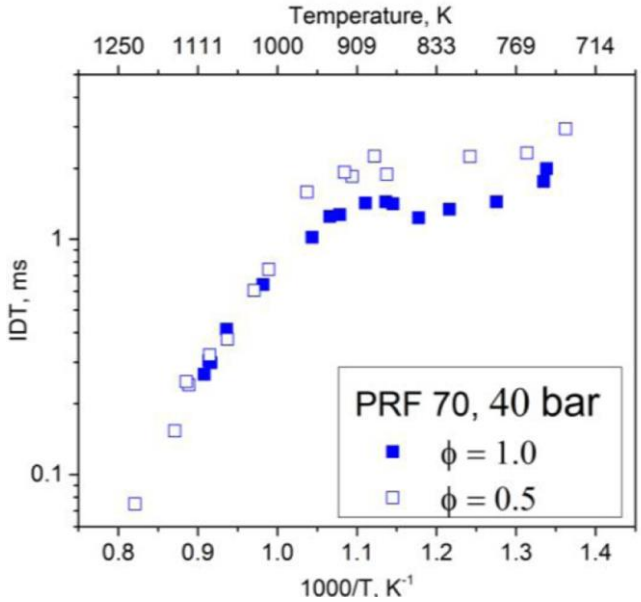

Figure 4: Influence of equivalence ratio on ignition delay times for PRF 70 at 40bar (from Ref. [8]).

2.4 Knock mitigation strategies

In this section, the knock mitigation strategies related to the results in our thesis are explained from Ref. [3].

2.4.1 Spark retardation and Octane Number

The few easiest ways to mitigate knock in an engine are retarding spark timing [22 - 23] and increasing the octane number [23] of the fuel. These methods can be implemented without any modifications to the engine. By retarding the spark timing, the pressure and temperature of the end-gas can be lowered. Lower end-gas temperature and pressure lead to increase in the ignition delay times and higher knock resistance. The downside to spark retardation is the possibility of an un-optimized combustion phase with lower thermal efficiency [24]. The octane number of the fuel can be achieved by additives like ethanol which are known to improve the knock resistance of the fuel.

2.4.2 Exhaust Gas Recirculation (EGR)

Exhaust gas recirculation (EGR) is an effective method for mitigating knock [22], [23], and [25]. Cooled EGR has the potential to supress knock without sacrificing the output power. This is possible as cooled EGR lowers the temperature in the cylinder allowing more fuel to be consumed before reaching the autoignition temperature. Higher percentage of EGR leads to a considerable increase in knock resistance and hence improved combustion phasing [26] and better operability at high loads.

Theoretically, EGR improves the thermal efficiency due to the increased ratio of specific heats and increased compression ratio and the reduction in combustion temperatures leading to lower heat transfer losses. However, using EGR without cooling has the opposite effect and increases the possibility of knock due to its higher temperature and should be avoided.

2.4.3 Cooling

From the above sections, we have established that higher temperatures lead to a higher possibility of knocking. Hence, reducing the temperature of the walls of the cylinder is also an effective approach to reduce the end-gas temperatures. Additionally, the effective temperature distribution of the cylinder wall has been proven to improve knock resistance [27] and this can be done by altering the flow of the coolant. However, if the heat transfer is increased, the thermal efficiency of the engine is lowered. Therefore, to mitigate knock without compromising the thermal efficiency, only the upper portion of the exhaust side bore should be cooled, and sufficient insulation should be provided to maintain the temperature of the centre and lower portions of the bore.

Another cooling method for knock mitigation would be to reduce the temperature of the charge during intake. From the Livengood-Wu integral, the initial temperature of the end-gas (charge intake) is very important in the autoignition temperature of the fuel. Higher initial temperatures lead to shorter ignition delay times.

2.4.4 Compression Ratio

Controlling the compression ratio in an engine is very important. A higher compression ratio has a higher possibility of knocking. A low cost and effective way to control the effective compression ratio in an engine is through Variable Valve

Timing (VVT). Additionally, Late intake valve closure (LIVC) is an effective method to lower the compression ratio of an engine at higher loads.

The more ideal approach would be to adopt a Variable Compression Ratio (VCR). This would make the engine structure a lot more complex and expensive [28].

2.5 Criteria for Knock prediction

As explained earlier, in this thesis, the software CHEMKIN-Pro will be used to validated various chemical kinetic models and the ignition delay times will be calculated.

In an engine, knocking in the high-torque and high-load region is of high importance. Low RPM allows for a longer window of time for the autoignition to occur and hence the chance and severity of the knock is higher. Hence in our thesis we will be using the experimental data by Kalghatgi et al. [7] in the low RPM and high load region to suggest the best operating conditions of the fuel under said engine conditions.

The aim of Ref. [7] was to compare the ignition delay times from the chemical kinetic mechanism and the experimental results. The ignition delay times for five different fuels at different temperatures and pressures were obtained from an experiment and were also calculated using chemical kinetic models (discussed in the coming sections). The fuel of importance to us is Fuel A from Table 1.

Fuel	Description	Average Chemical Formula	*RON*	*MON*
A	Face Fuel F	$C_{6.7}H_{13.8}$	94.1	87.5
B	Face Fuel G	$C_{7.1}H_{12.84}$	96.7	86
C	Face Fuel G + 7% n-heptane	$C_{7.09}H_{13.0}$	91.9	83.8
D	Face Fuel G + 10% Ethanol	$C_{6.1}H_{11.5}O_{0.2}$	99.1	87.0
E*	PRF 87 + 20% Ethanol	$C_{5.45}H_{12.9}O_{0.4}$	101.8	93.7

* 69.6% v iso-octane+ 10.4%v n-heptane + 20% v ethanol

Table 1: Composition of the fuels tested in Ref. [7].

The results from the chemical kinetic mechanism of Fuel A were fitted using the following simple equation.

$$\tau_i = A exp\left(\frac{B}{T}\right) P^{-n} \quad 4$$

Where A, n, and B are parameters that vary depending on the RON and S of the fuel. These parameters were calculated for a wide range of RON (88-100) and S (8-12) were calculated in Ref. [29].

These theoretical calculations were compared to the results from the experiment using a single cylinder engine at King Abdullah University of Science and Technology. Fuel A ran at different spark timings for condition 1 mentioned in Table 2.

Cond.	Speed, *RPM*	Intake Temp. °C (Tin)	Intake Pr. KPa abs. (Pin)	Mean bulk T_{comp15} K	ΔT K. temp increment in hot spot at 15 bar*
1	1500	30	102.0	685	10
2	1500	65	102.0	713	10
3	1500	30	165.0	590	30

Table 2: Fuel operating parameters.

Further, to account for the cyclic variations in an actual engine, the knock onset prediction for four different cycles was calculated.

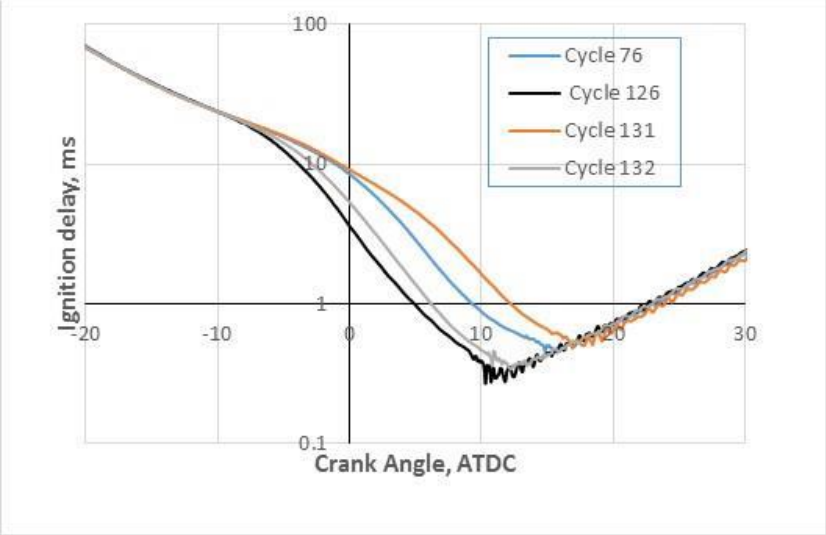

Figure 5: Ignition delay times as a function of crank angle degrees for cyclic variations from Ref. [7].

The ignition delay times corresponding to the four different cycles shown in Figure 5. were calculated using equation 4 and the predicted positions of knock onset agreed well with the knock signal to within 1 Crank Angle Degree (CAD).

From the above discussion, we can observe that in Ref. [7] (experimental data and the knock prediction model), knock appeared when the ignition delay time was longer than an average of **0.5ms** for a fuel of RON ~ 95 and at low RPM and high load. This criterion was chosen to predict the best operating range for the fuels in our thesis using the ignition delay times computed using the selected mechanism.

3 Research Method

Knowing the temperature, pressure, and the mixture composition, we can use the computational tool Chemkin-Pro to calculate the ignition delays of different fuels. The basic method of calculating ignition delays can be found in the Chemkin Theory Manual [30]. We will explore three state-of-the-art chemical mechanisms for different fuel/fuel blends and assess them using recent experimental data. Then, a mechanism suitable for subsequent study will be selected.

3.1 Chemkin-Pro

3.1.1 Prerequisites

To run a project on Chemkin-Pro, two input files are required. These two files are *chem.inp* and *therm.dat.* The file *chem.inp* contains all the data necessary on the fuel species, chemical reactions and reaction pathways. The file *therm.dat* contains the thermodynamic data for all chemical species included in a reaction mechanism. More details can be found in the Chemkin-Pro getting started manual [31]. The input files for the mechanisms adopted in the present work were uploaded as supplementary materials to the respective papers.

Since Chalmers has multiple licences for ANSYS 2020 (Chemkin-Pro is a part of ANSYS) and the system we worked with had 6 cores in the processor, we were able to run 6 simulations in parallel. These settings can be found in Home>Edit>Preferences>Run/Output as shown in Figure 6.

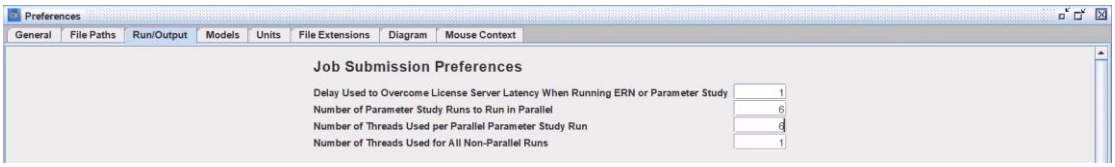

Figure 6: Chemkin-Pro settings to control parallel simulations.

Another preference which needs to be changed to run multiple simulations is the *ckjavamemory.* The default value on a 64-bit Windows machine is 1024Mb (1Gigabyte) which is very low and this needs to be changed. A higher value of *ckjavamemory* is essential as our simulations involve a large parameteric study and complex reaction pathways. There are two different types of memory consumption and they are: starting memory consumption and maximum memory consumption. To change these values, a file called "run_chemkinpro_env_setup.bat" should be located in the following path: 'C:\\ Ansys Inc \ (version of ANSYS) \ reaction \ chemkinpro.win64\bin'. The file should then be opened using notepad with administrative privileges. On further examination of the notepad, the values in SET **CKJAVAMEMORY**=-Xms16g -Xmx16g should be changed to the required memory values. Here, Xms stands for starting memory and Xmx stands for maximum memory. Care has to be taken to ensure the syntax is correct as it is case sensitive. In our case, we kept both these values same and at 16Gigabytes which enabled us to run our simulations at a higher speed. The only downside to keep both these values same is the start-up time of the Chemkin-Pro software increased slightly. More information can be found in the getting started manual [31].

3.1.2 Project setup

In this section, we describe the process of setting a project and various input parameters and reasons for choosing them.

3.1.2.1 Reactor model

We first chose the closed homogeneous batch reactor as our reactor model in which to run the simulation. This is chosen as it gives the user a lot of flexibility to study the ignition delay times for a fuel without having to specify the operating parameters of an engine/turbine. In this thesis we only use the ignition delay times to study the auto-ignition of fuels and therefore some important input parameters for us are simulation time, error tolerances, volume, temperature, pressure, equivalence ratio and fuel composition (and in some cases the exhaust gas recirculation percentage).

3.1.2.2 Chemistry set (Chemical mechanism)

Here, we first select the working directory in which we have the input files and also where we need to save our simulations. We then choose the **GAS-Phase Kinetics File** (which is the *chem.inp*) and the **Thermodynamics Data File** (which is the *therm.dat*) and save the mechanism with the required name and run the pre-processor as seen in Figure 7. The mechanism is the saved as a *.cks* file.

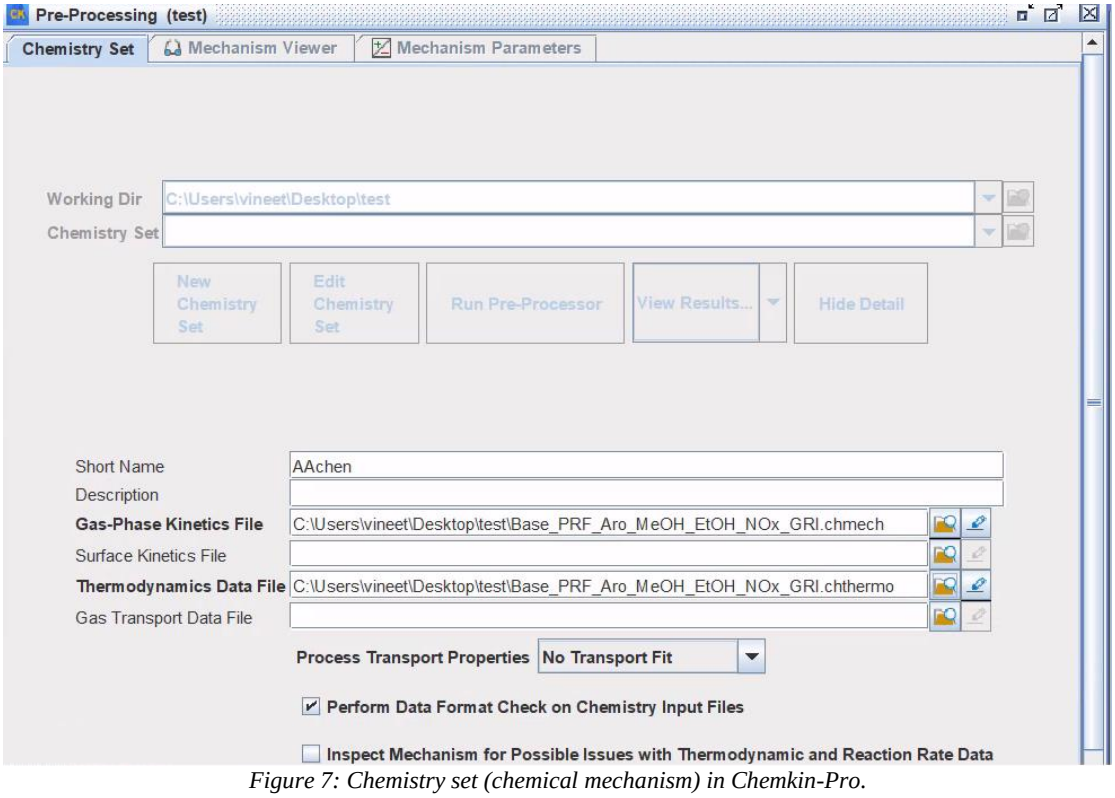

Figure 7: Chemistry set (chemical mechanism) in Chemkin-Pro.

3.1.2.3 Reactor Physical Properties and Reactant Species

Once the pro-processor is run, we move on to input various parameters of these simulations in the reactor. We first choose the problem type as Constrain Volume and Solve the energy equation as an SI engine (Otto cycle) in a constant volume cycle. The end time is chosen as 0.01 seconds to ensure we provide enough time for the

combustion to occur. We choose the starting temperature as 600K and pressure as 5bar. The volume is chosen as 1cm^3 as stays constant throughout the reaction Figure 9.

Since most of the fuel blends mention the volume % of the additives (ethanol), Kalghatgi et al. [5] developed a method to calculate the mole % of each component in a fuel blend. A screenshot showing the calculation for E10 is shown in Figure 8.

Inputs	
RON of Base Fuel	85
Sensitivity of Base Fue	0
Ethanol (vol%)	10%
Base Fuel vol%	
iso-octane (vol%)	85,0%
n-heptane (vol%)	15,0%
toluene (vol%)	0,0%
TMF (mole%)	0,0%
Fuel mole%	
iso-octane (mole%)	63,8%
n-heptane (mole%)	12,6%
toluene (mole%)	0,0%
ethanol (mole%)	23,6%

Calculated from: G. Kalghatgi et al./ SAE Int J Eng 8 (2015) 505–19

Outputs Linear Model	
Predicted RON	94,6
Predicted MON	89,7
RON Calculation Linear Model	
Transition Point	0,08
D	7,33
a	-34,32
b	59,93
c	82,39
toluene effect	0,00
MON Calculation Linear Model	
Transition Point	0,05
D	5,25
a	-23,07
b	29,83
c	83,93
toluene effect	0,00

Outputs Non-Linear Model	
Predicted RON	93,3
Predicted MON	89,8
RON Calculation Non-Linear Model	
Transition Point	0,14
D	7,33
a	-39,68
b	68,25
c	79,42
toluene effect	0,00
MON Calculation Non-Linear Model	
Transition Point	0,04
D	5,25
a	-22,55
b	29,04
c	84,21
toluene effect	0,00

Figure 8: Screenshot of the fuel component calculation for PRF-Ethanol blend of RON95 from Ref. [5].

In the reactant species tab, we choose the starting equivalence ratio as 0.5. Using the fuel calculation from [5] we calculate the mole% of iso-octane to be 94.4% and n-heptane to be 5.6% for a PRF fuel of RON95. In the Oxidizer mixture tab, we select auto-populate air and in the Complete-combustion products tab we select auto-populate.

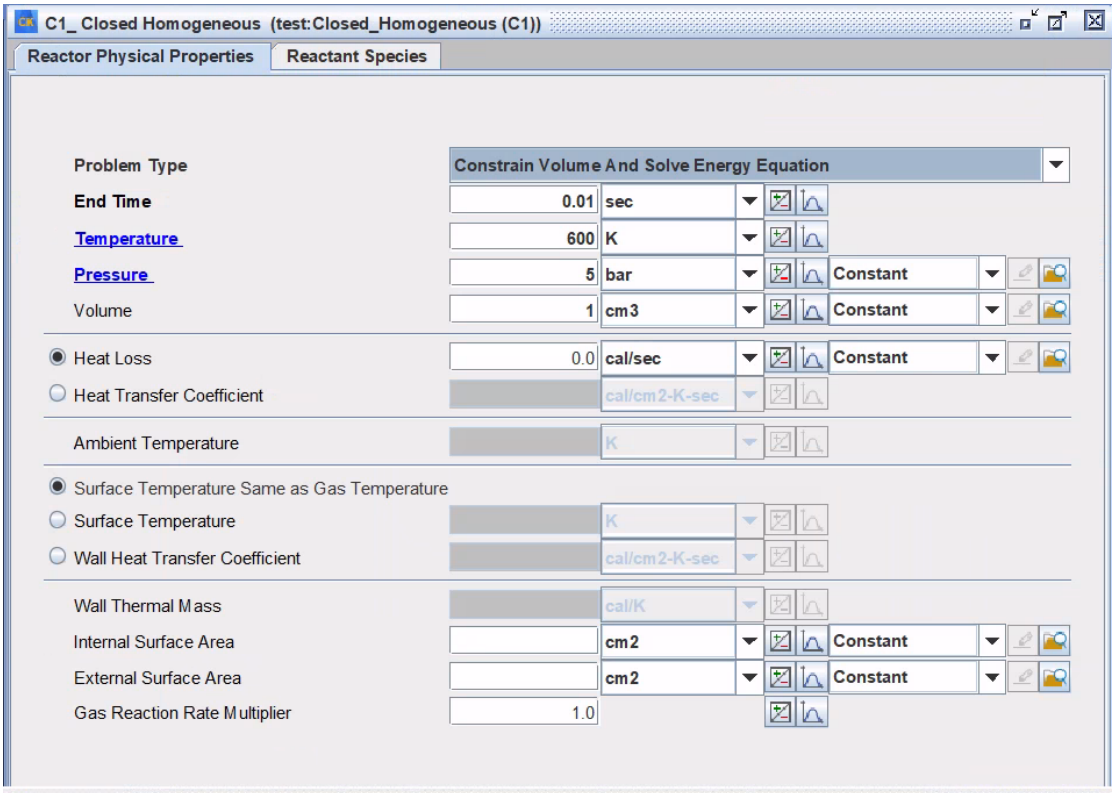

Figure 9: Input parameters in the reactor model.

As we want to run multiple simulations with a single setup, we perform a parametric study for temperatures, pressures, and the equivalence ratios as below:

- Temperature : 600K – 1400K (increments of 10K)
- Pressure : 5bar, 10bar, 20bar
- Equivalence ratio : 0.5, 1, 1.5

The results of these simulations are discussed in the later sections.

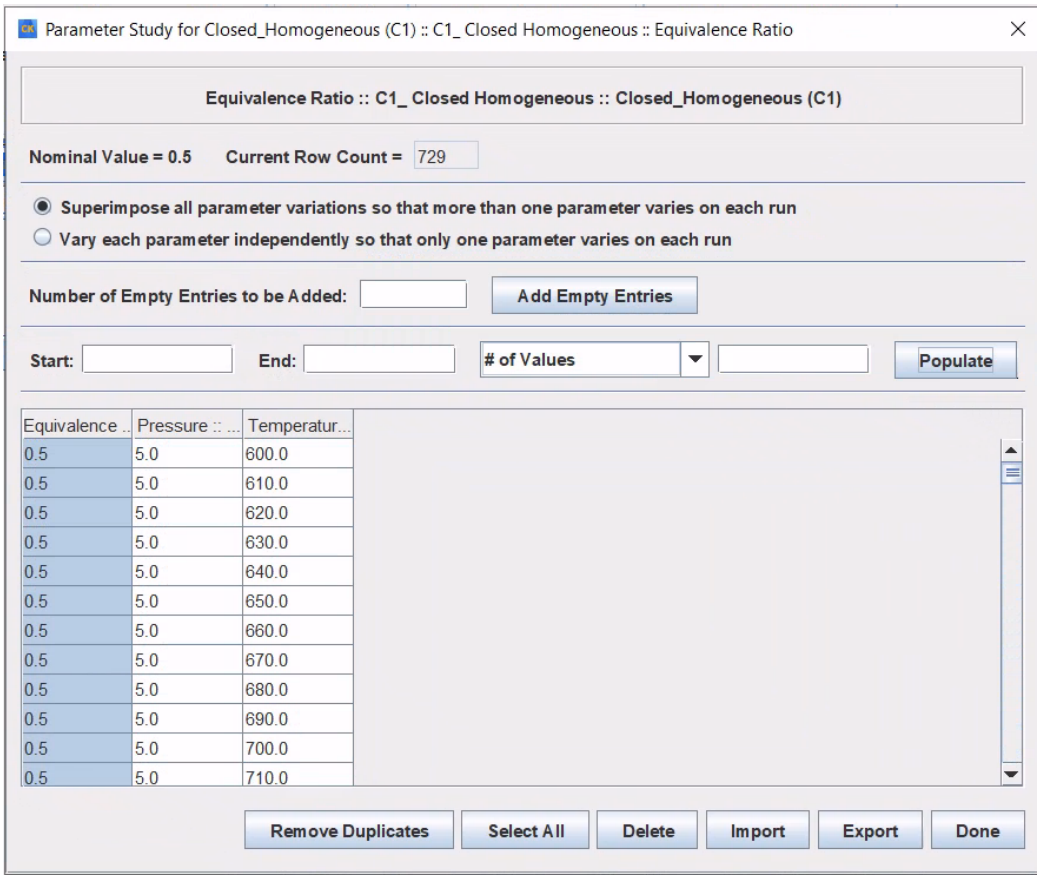

Figure 10: Parameter study for various temperatures, pressures and equivalence ratios.

The project is then saved and file with the extension *.ckprj* is created.

3.1.2.4 Reaction Workbench

After saving our project, we click on 'View in reaction workbench' to start our simulation. We then choose the working directory and select the previously saved *.ckprj* file as the initial CHEMKIN project. Figure 11 shows the various settings in the reaction workbench (various tabs above) and the number of simulations to be run.

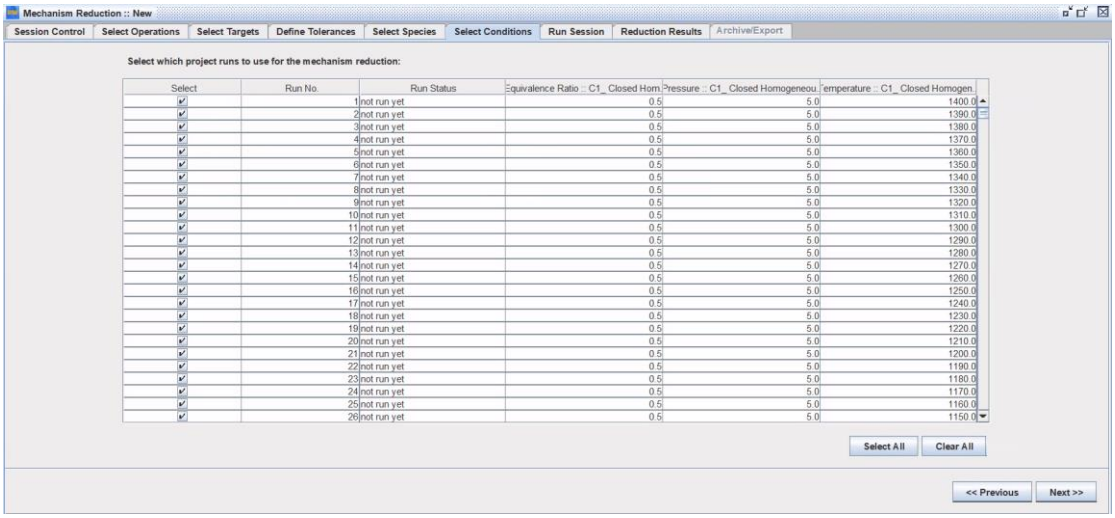

Figure 11: Settings in the reaction workbench (the various tabs above) and the number of simulations to be run.

After the simulation runs, we get the results shown in Figure 12.

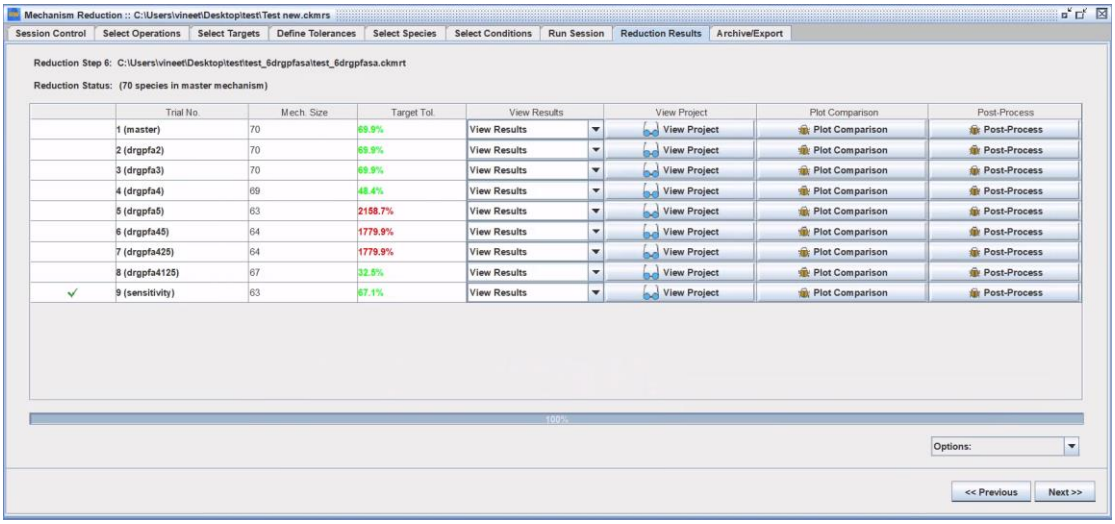

Figure 12: Results of a mechanism reduction.

Chemkin-Pro has a wide range of post-processing tools available to plot the results from the simulations. However, it is extremely difficult and almost impossible to plot the results we need. Therefore, we used Excel to post-process the data obtained from simulations and we used MATLAB and Excel to plot the graphs according to our specifications.

3.2 Calculation of Ignition Delay Time

The close homogeneous batch reactor model can be used to study the auto-ignition of a fuel using various criteria such as the heat release during the combustion process (indicated by the inflection point in the temperature profile) or concentrations of certain species at any given point in the combustion process. Moreover, the reactor model allows us to study the ignition delay times at various temperatures, pressures, and equivalence ratios.

The volume in the reactor is kept constant and the energy equation is solved to study the ignition delay times with respect to the set variables and the end time of the simulation should be chosen to provide sufficient time for combustion to take place.

In the output control setting of the reactor model, under the Ignition Delay tab, a check box for Temperature Inflection Point is found and this needs to be checked for us to get the ignition delay times in the output of the simulation. Where the temperature inflection point is defined as the time at which the rate of change of temperature as a function of time reaches a maximum. When selected, the ignition delay time is calculated as the time when the slope of the temperature profile reaches a maximum value. Figure 13. shows a typical knock case where the knock is observed at a CAD of CA_{ko}. At this CAD, the unburned gas temperature is the highest and the Heat Release Rate (HRR) is highest and as stated before, this point would be the maximum rate of change of temperature in the combustion process and is the temperature inflection point.

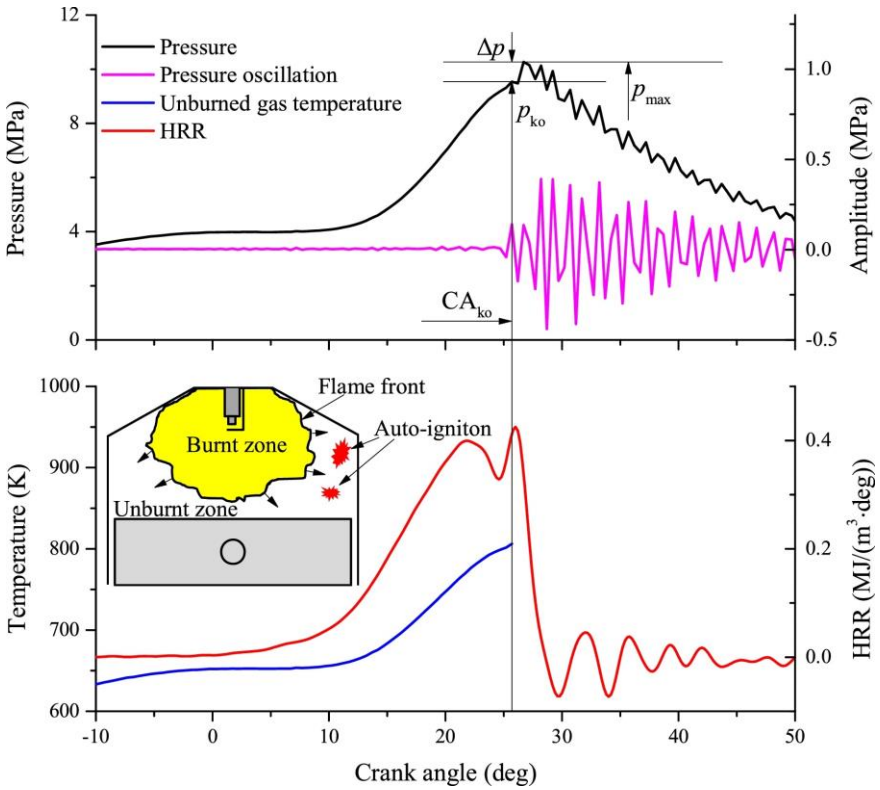

Figure 13: A typical knocking case (from Ref. [3])

A parametric study for temperature, pressure, equivalence ratio and EGR are set up to study the dependence of the ignition delay time on these parameters. Only one of these parameters varies on each turn.

After the reactant species are chosen, the next step is to select the target parameters of the simulation (since the temperature inflection point was selected in output control, we get the option to study the ignition delay time) which is the ignition delay time. The tolerances for the target parameters need to be defined and the absolute tolerance is set to 10^{-6} and the relative tolerance to 10%. The output also the option of selecting the end-point value or the maximum value. The ignition time is selected to show the end-point value.

If necessary, other output parameters like the emissions (NO_x, CO, CO_2) can be chosen to study their influence/relationship with the ignition delay times.

In our thesis the temperature inflection point is chosen as the criteria to study knocking. Alternatively, for the same problem type of constant volume and solving the energy equation (at fixed parameters), the following criteria can be used to study autoignition:

- Time at which the concentration of certain species like emissions reach their maximum value.
- Time at which the concentration of the radical OH reaches its maximum value.
- By selecting the option “Integrate Heat Release by Gas-Phase Reactions” in the output control to solve a separate equation to integrate the heat release due to gas-phase reactions to obtain a more accurate heat-release profile.

- The time at which a specified rate of increase of temperature occurs. This can be achieved by setting the ignition temperature threshold to determine when ignition occurs and allows CHEMKIN-Pro to print the ignition delay times based on this threshold.

3.3 Mechanisms

3.3.1 RWTH Aachen University [32]

The kinetic model for PRF mixtures proposed in Ref. [32] was developed from the mechanism published mechanism by Curran et al. [33]. The detailed oxidation chemistries of n-heptane and iso-octane are captured in Ref. [33] and it has been validated for various experimental configurations. To further reduces the computational time and effort, the detailed mechanism was first reduced to a skeletal level using a multi-stage reduction strategy [34]. The reduction process and the error propagation algorithm ensure that there is minimal effect. Even though Ignition Delay times are not targets directly, they are not altered by accurate predictions of the chemistry of the target species. The authors observed a maximum deviation of about 5% compared to the experimental data [35-36].

3.3.2 King Abdullah University of Science and Technology (KAUST) [37]

In the previous study by KAUST [38], a three-component toluene primary reference fuel (TPRF is a combination of toluene, iso-octane and n-heptane) kinetic model was developed and fully validated. The goal of Ref. [37] was to develop a four-component toluene primary reference fuel with ethanol (TPRF-E) model with a lesser species count and reactions. The model includes low, intermediate and high-temperature chemistry in normal engine combustion. With a list of important starting species, the remaining species which do not play a part in the reaction pathways are removed based on the user defined maximum error setting. Additionally, the important input parameters of interest, like the equivalence ratios, temperature and pressure are specified. In Ref. [37], targeted conditions for reduction include high/low temperatures (600–1300 K), high pressures (5–50 atm); lean to reach equivalence ratios and the error for heat release is specified as 0.5.

3.3.3 Lawrence Livermore National Laboratory (LLNL) [39]

This chemical kinetic model is based on the previous works carried out by the LLNL research group. The general structure of the mechanisms includes the detailed mechanism of C1-C4 group and three other main blocks. First block: main reactions pathways of linear hydrocarbons up to C7. Second block: reactions for branched hydrocarbons from C5 to C8. Third block: reactions of aromatic structures. All the interactions between the oxidation pathways of various components were accounted for by the reactions of smaller radicals.

In the recent times, significant revisions of some important reaction rates included in the mechanism have been carried out. A thorough revision of the latest recommendations for many of these reaction rates allowed the performance of the model to be improved over a wide range of operating conditions.

4 Results and Discussion

4.1 Validation of mechanisms

4.1.1 n-Heptane

The experimental data on the ignition delay times for the following parameters were chosen from Ref. [10] and are as follows:

- Temperature range (T): 600K – 1500K
- Pressure (P): 13bar and 40bar
- Equivalence ratio (EQR/ϕ): 0.5, 1 and 2

Figures 14 – 19 report the results computed using the Aachen mechanism [32] and the KAUST mechanism [37] and its comparison with the experimental data taken from Ref. [10].

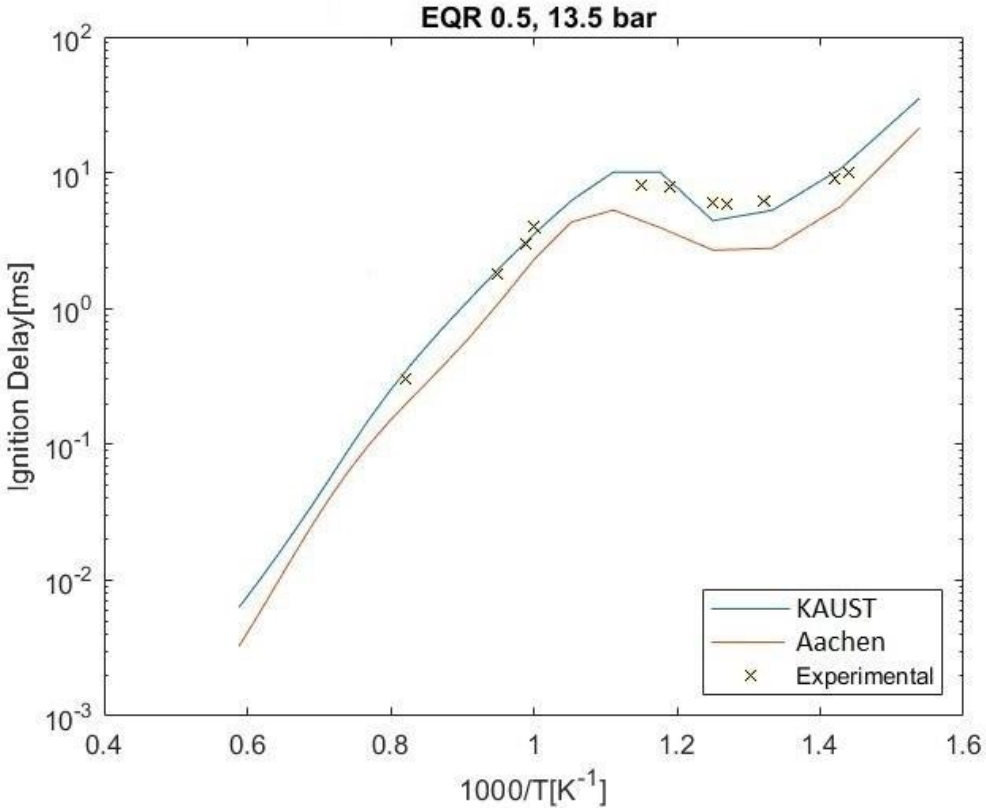

Figure 14: Ignition delay times of n-heptane/air mixtures for ϕ = 0.5 and pressure of 13.5bar. Symbols show the experimental data [10]. Blue and brown solid lines show results computed using KAUST [37] and Aachen [32] mechanisms, respectively.

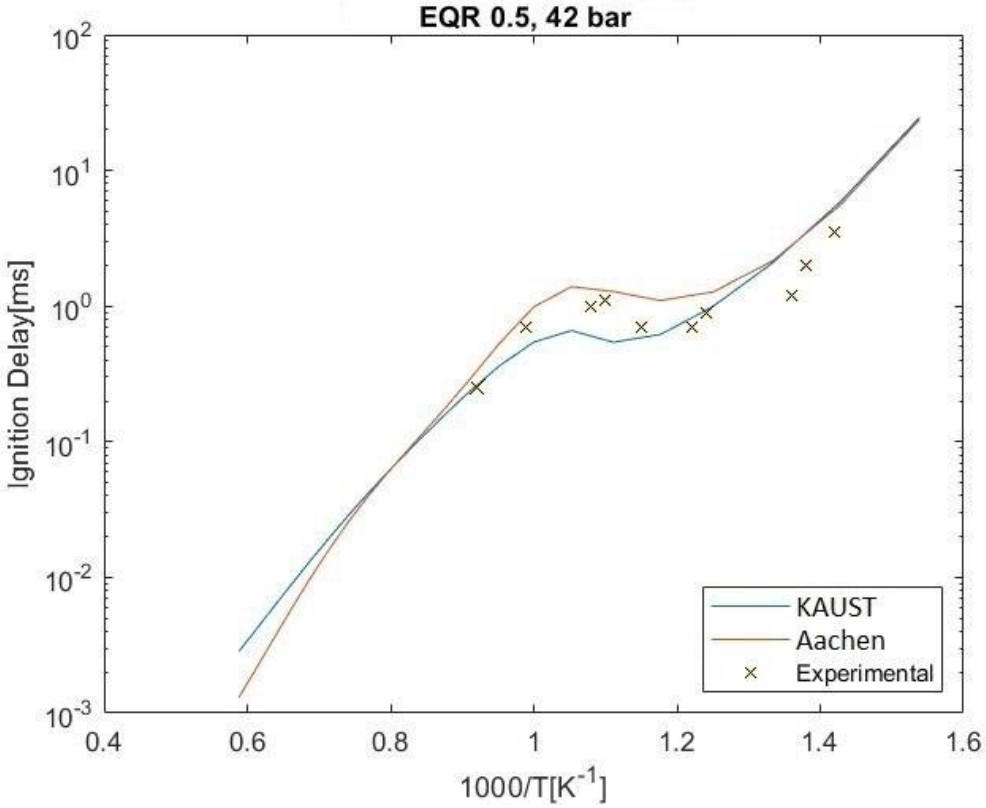

Figure 15: Ignition delay times of n-heptane/air mixtures for ϕ = 0.5 and pressure of 42bar. Symbols show the experimental data [10]. Blue and brown solid lines show results computed using KAUST [37] and Aachen [32] mechanisms, respectively.

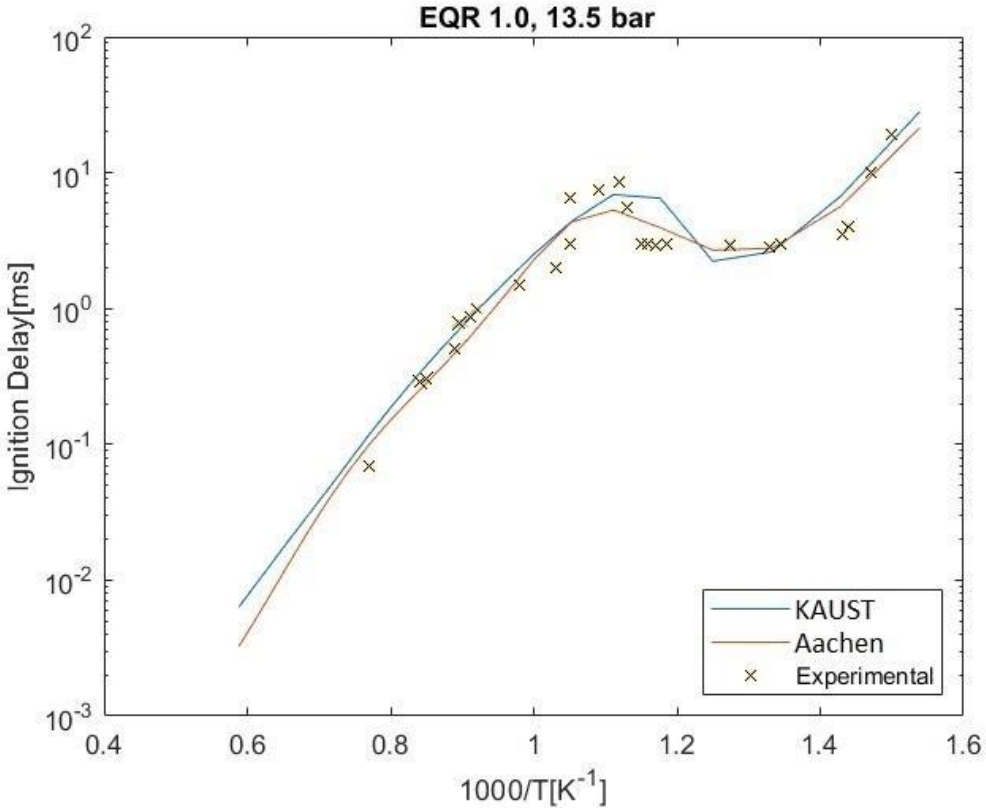

Figure 16: Ignition delay times of n-heptane/air mixtures for ϕ = 1 and pressure of 13.5bar. Symbols show the experimental data [10]. Blue and brown solid lines show results computed using KAUST [37] and Aachen [32] mechanisms, respectively.

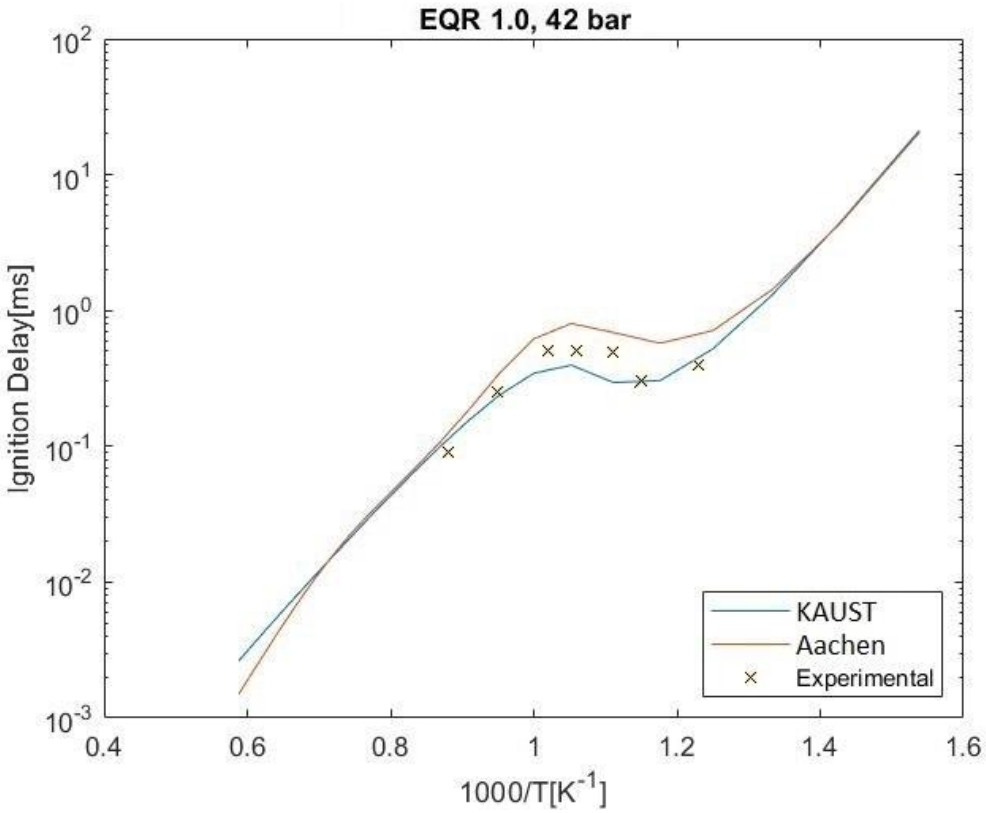

Figure 17: Ignition delay times of n-heptane/air mixtures for ϕ = 1 and pressure of 42bar. Symbols show the experimental data [10]. Blue and brown solid lines show results computed using KAUST [37] and Aachen [32] mechanisms, respectively.

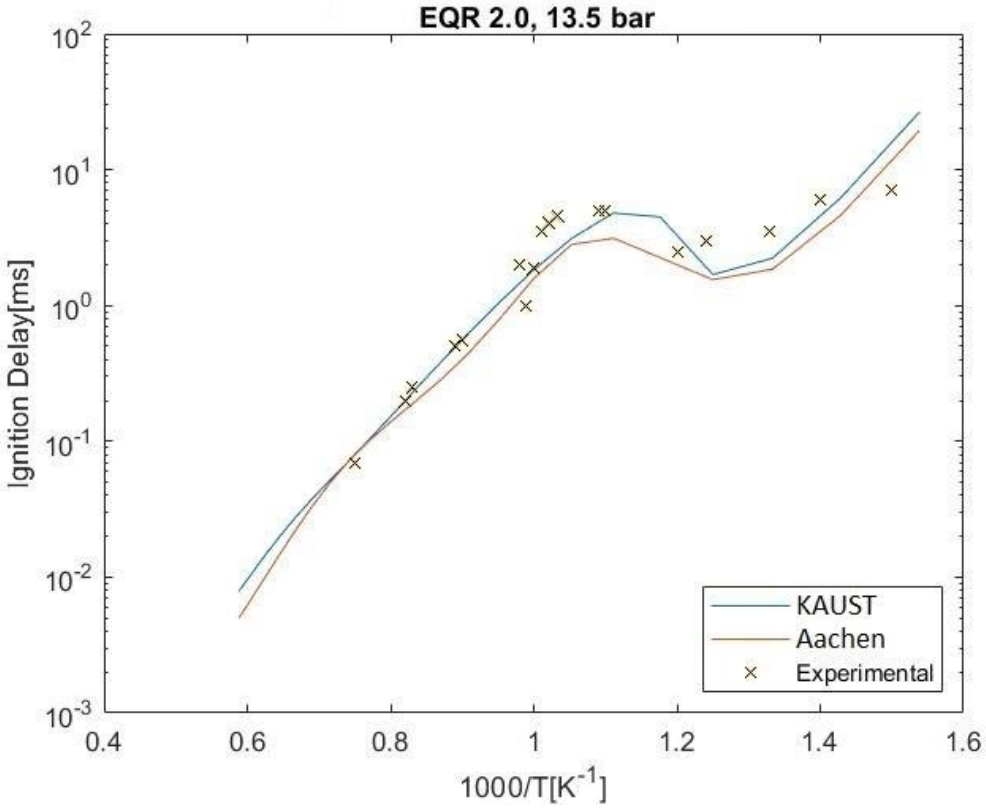

Figure 18: Ignition delay times of n-heptane/air mixtures for ϕ = 2 and pressure of 13.5bar. Symbols show the experimental data [10]. Blue and brown solid lines show results computed using KAUST [37] and Aachen [32] mechanisms, respectively.

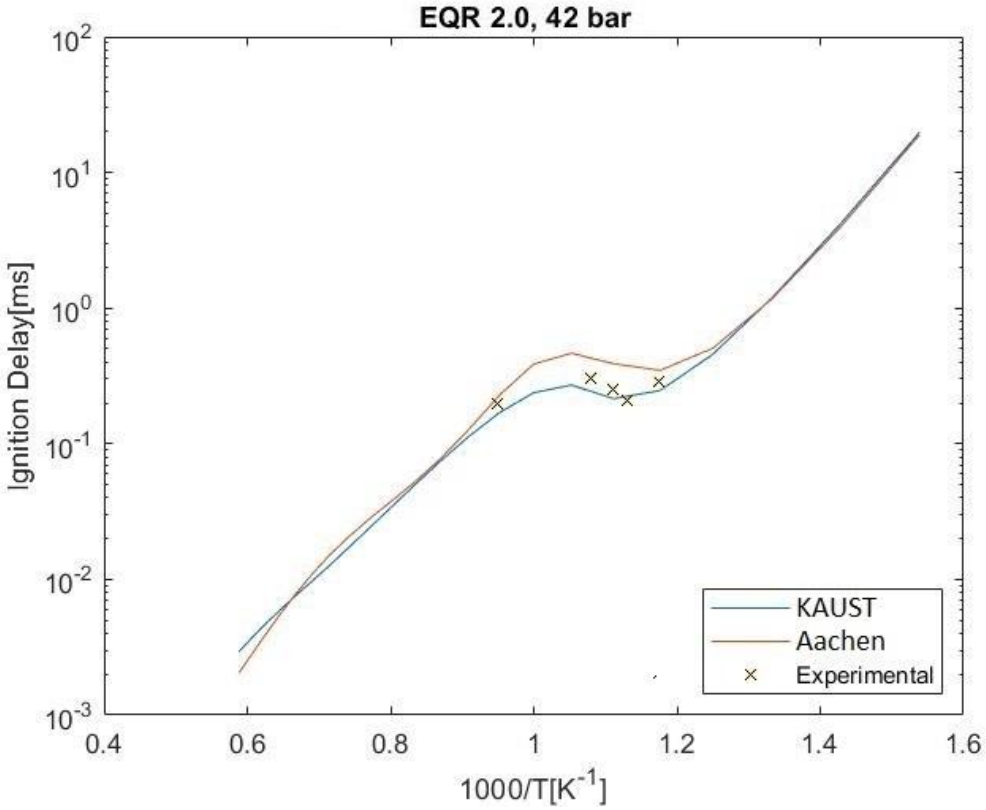

Figure 19: Ignition delay times of n-heptane/air mixtures for ϕ = 2 and pressure of 42bar. Symbols show the experimental data [10]. Blue and brown solid lines show results computed using KAUST [37] and Aachen [32] mechanisms, respectively.

Figures 17 - 22 reports ignition delay times vs inverse temperature at ϕ = 0.5, 1 and 2 at 13.5 and 42bar pressure. The blue and brown lines show results computed using the KAUST mechanism [37] and the Aachen mechanism [32], respectively and symbols show the experimental data taken from Ref. [10].

- Both mechanisms yield comparably good results across all temperatures at 13.5 bar pressure and for ϕ = 1 and 2.
- Both mechanisms yield comparably poor results in the NTC region at 42 bar pressure and for ϕ = 0.5
- KAUST mechanisms [37] performs better than the Aachen mechanism [32] across all temperatures at 13.5 bar pressure and ϕ = 0.5.
- Aachen mechanism [32] performs better than the KAUST mechanism [37] in the NTC region at 42 bar pressure and for ϕ = 1 and 2.

When using the Aachen mechanism [32], the computation time was larger by approximately 20% when compared to the time required to perform the same simulations using the KAUST mechanism [37].

4.1.2 iso-Octane (IC8H18)

The experimental data on the ignition delay times for the following parameters were chosen from Ref. [53]:

- Temperature range (T): 600K – 1500K
- Pressure (P): 13.5bar and 42bar
- Equivalence ratio (EQR/ϕ): 0.5, 1 and 2

Figures 20 – 22 report the results computed using the Aachen mechanism [32] and the KAUST mechanism [37] and its comparison with the experimental data taken from Ref. [40].

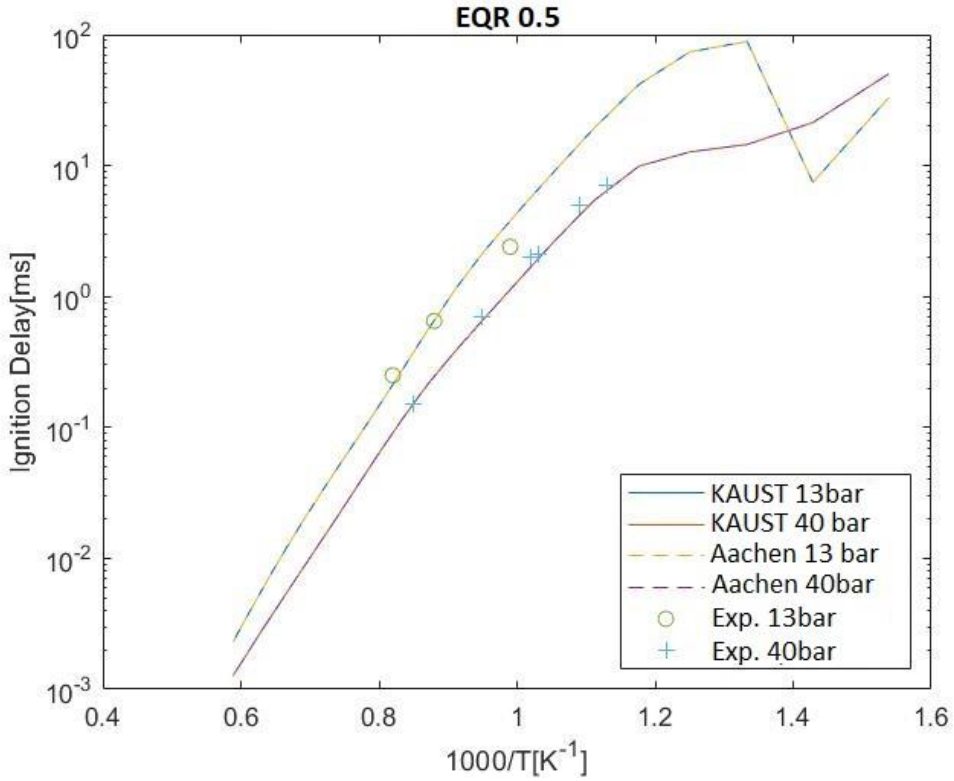

Figure 20: Ignition delay times of iso-octane/air mixtures for ϕ = 0.5 and pressures of 13bar and 42bar. Symbols show the experimental data [41]. Blue and brown solid lines show results computed using KAUST [37] mechanism at 13bar and 40bar pressures, respectively. Yellow and purple dashed lines show results computed using Aachen [32] mechanism at 13bar and 40bar pressures, respectively.

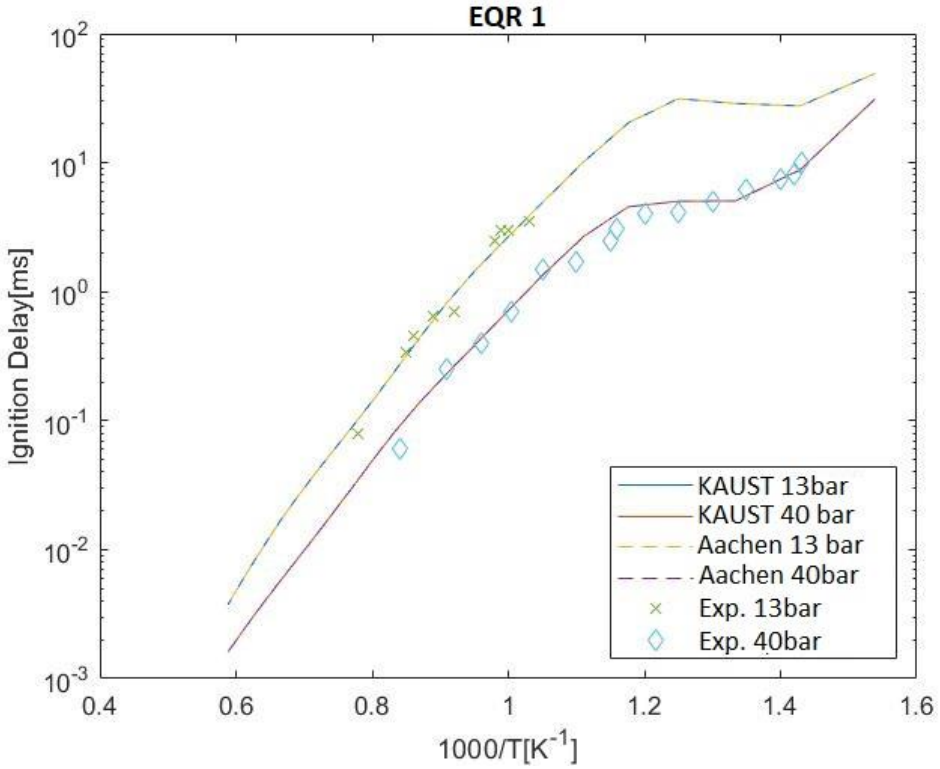

Figure 21: Ignition delay times of iso-octane/air mixtures for ϕ = 1 and pressures of 13bar and 42bar. Symbols show the experimental data [41]. Blue and brown solid lines show results computed using KAUST [37] mechanism at 13bar and 40bar pressures, respectively. Yellow and purple dashed lines show results computed using Aachen [32] mechanism at 13bar and 40bar pressures, respectively.

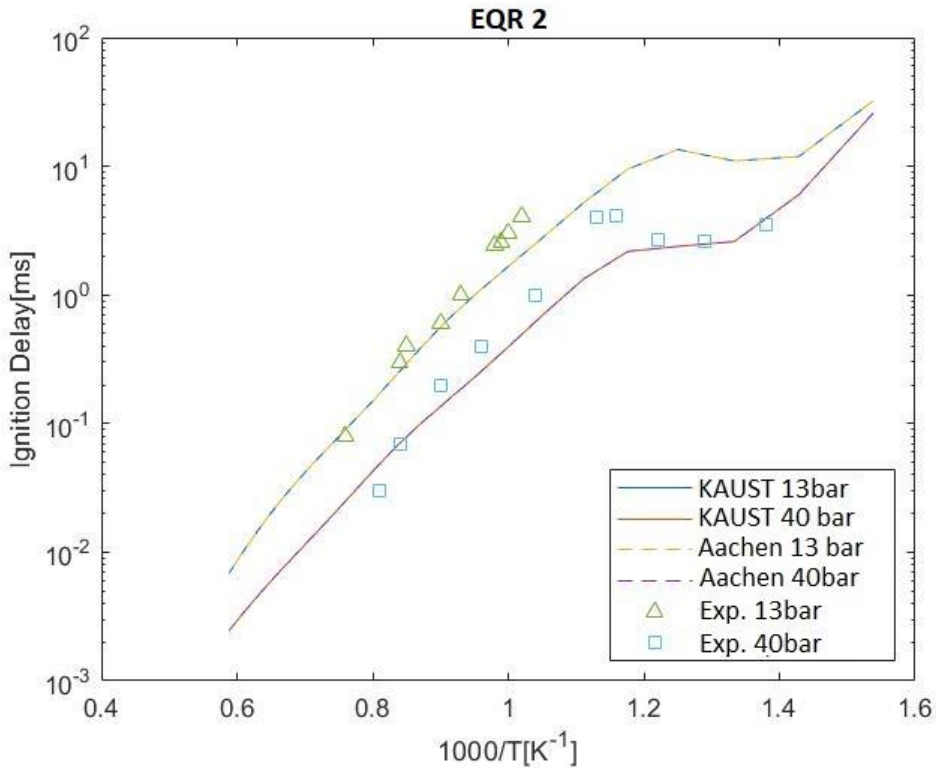

Figure 22: Ignition delay times of iso-octane/air mixtures for ϕ = 0.5 and pressures of 13bar and 42bar. Symbols show the experimental data [41]. Blue and brown solid lines show results computed using KAUST [37] mechanism at 13bar and 40bar pressures, respectively. Yellow and purple dashed lines show results computed using Aachen [32] mechanism at 13bar and 40bar pressures, respectively.

Figures 20 - 22 reports ignition delay times vs inverse temperature at ϕ = 0.5, 1 and 2 and at 13bar and 40bar pressures where the blue and brown lines show results computed using the KAUST mechanism [37] at 13bar and 40bar, respectively, yellow and purple dashed lines show results computed using the Aachen mechanism [32] at 13bar and 40bar pressures, respectively and symbols show the experimental data taken from [53].

- Both mechanisms yield comparably good results at all the pressures and ϕ.

When using the Aachen mechanism [32], the computation time was larger by approximately 20% when compared to the time required to perform the same simulations using the KAUST mechanism [37].

4.1.3 PRF-Ethanol Mixture

The experimental data on the ignition delay times for the following parameters were chosen from Ref. [41]:

• Temperature range (T): 600K – 1500K
• Pressure (P): 10bar, 30bar and 50bar
• Equivalence ratio (EQR/ϕ): 1

Figures 23 – 25 reports the results computed using the Aachen mechanism [32], KAUST mechanism [37] and the LLNL mechanism [39] and its comparison with the experimental data taken from Ref. [41].

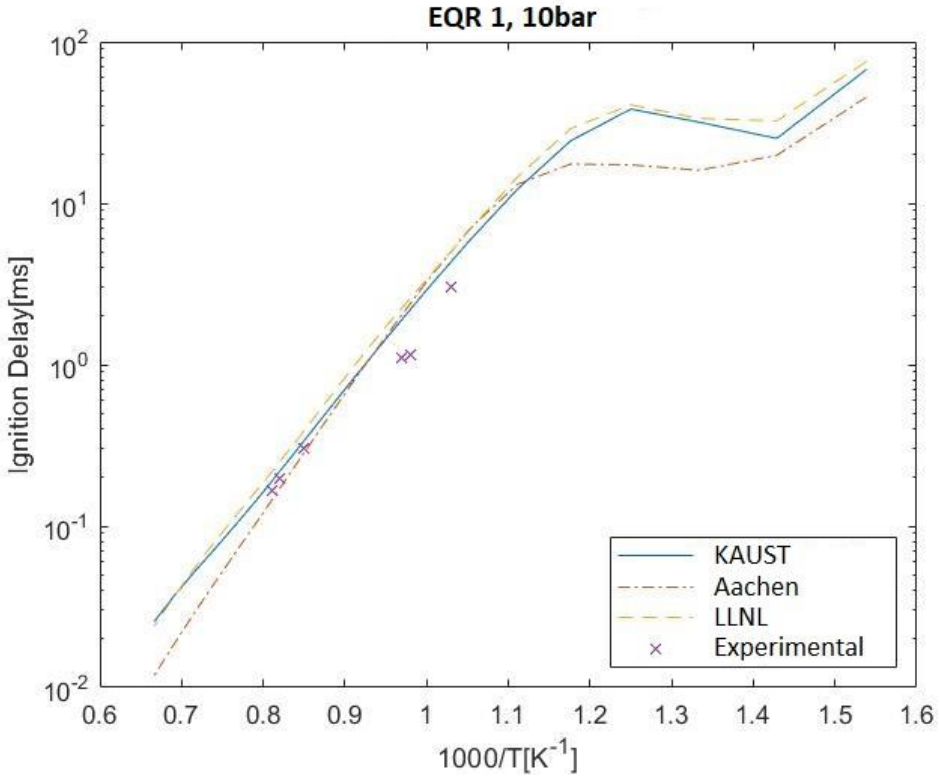

Figure 23: Ignition delay times of PRFE/air mixtures for ϕ = 1 and pressure of 10bar. Symbols show the experimental data [42]. Blue solid line, brown dot-dash line and yellow dashed line show results computed using KAUST [37], Aachen [32] and LLNL [39] mechanisms, respectively.

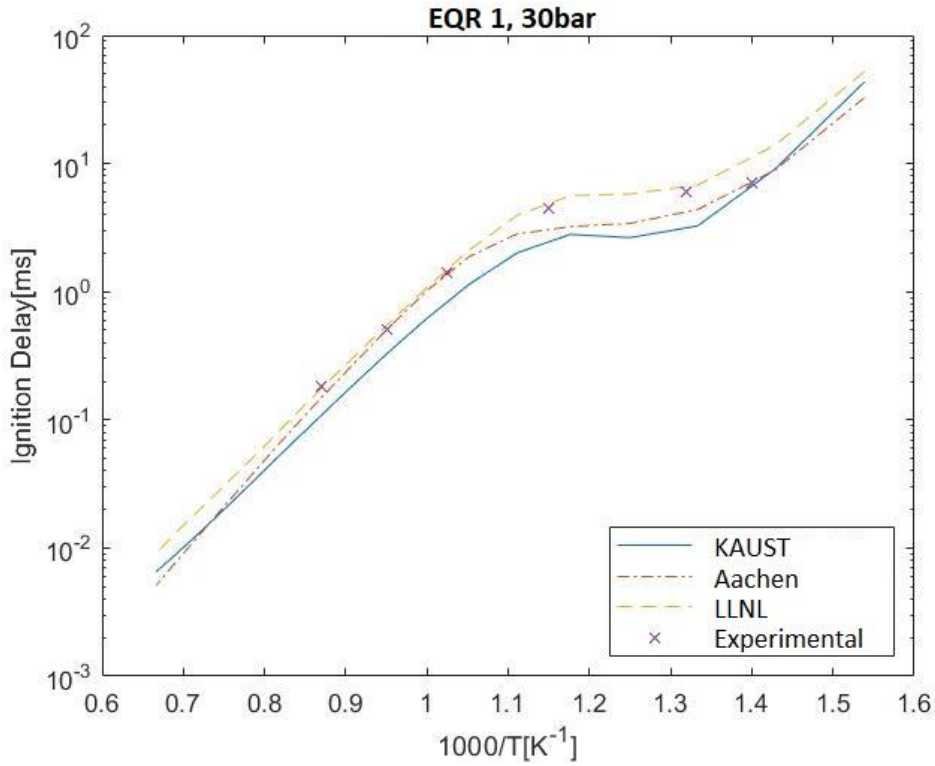

Figure 24: Ignition delay times of PRFE/air mixtures for ϕ = 1 and pressure of 30bar. Symbols show the experimental data [42]. Blue solid line, brown dot-dash line and yellow dashed line show results computed using KAUST [37], Aachen [32] and LLNL [39] mechanisms, respectively.

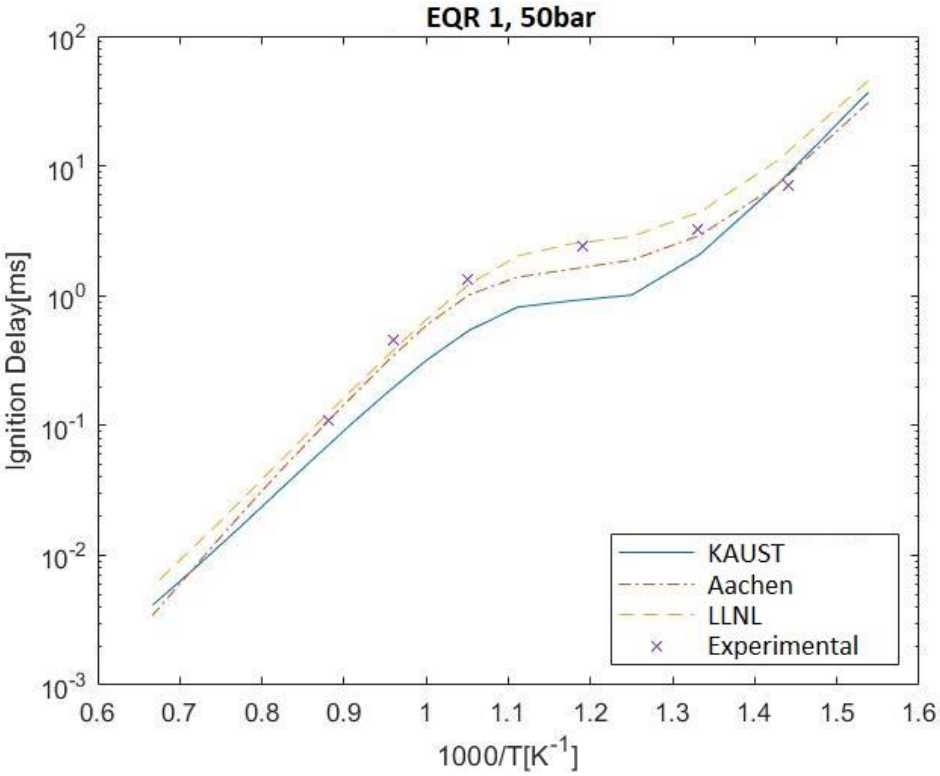

Figure 25: Ignition delay times of PRFE/air mixtures for ϕ = 1 and pressure of 50bar. Symbols show the experimental data [42]. Blue solid line, brown dot-dash line and yellow dashed line show results computed using KAUST [37], Aachen [32] and LLNL [39] mechanisms, respectively.

Figures 23 – 25 reports ignition delay times vs inverse temperature at $\phi = 1$ and 10bar, 30bar and 50bar pressures where blue solid line, brown dot-dashed line and yellow dashed line show results computed using the KAUST [37], Aachen [32] and LLNL [39] mechanisms, respectively, and the symbols show the experimental data taken from Ref. [42].

- All three mechanisms yield comparably good results at 10bar pressure and $\phi = 1$ across all the temperatures.
- Both LLNL [39] and Aachen mechanisms [32] yield comparably good results at 30bar and 50 bar pressures and at $\phi = 1$ in the high and low temperatures regions.
- The LLNL mechanism [39] performs better than the KAUST [37] and Aachen mechanisms [32] in the NTC region at 30bar and 50bar pressures and at $\phi = 1$.
- The KAUST mechanisms [37] performs poorly across all the temperature regions for 30bar and 50 bar pressures at $\phi = 1$.

When using the LLNL mechanism [39], the computation time was larger by approximately 20% when compared to the time required to perform the same simulations using the Aachen mechanism [32]. When using the latter mechanism, the computation time was larger by approximately 20% when compared to the time required to perform the same simulations using the KAUST mechanism [37].

4.2 Selection of Mechanism

Since the chosen LLNL mechanism [39] is only for multi-component fuels, it cannot run simulations for pure components i.e single components (Iso-octane and n-Heptane). LLNL has separate mechanisms for a wide range of single component fuels. Therefore, the results computed using this mechanism yielded results with a very high error margin and were not plotted for n-heptane and iso-octane. From the above plots, the KAUST mechanism [37] has the lowest deviation from the experimental values for n-heptane and has the lowest computation time.

For iso-octane, the results from the Aachen mechanism [32] and the KAUST mechanism are identical. However, when comparing the computation time, the KAUST mechanism would be the preferred option.

Finally coming to the PRFE simulation, which are of the highest interest in this paper, it is observed that the results from the KAUST mechanism have the highest deviation from the experimental data. In Figure 23, Figure 24, and Figure 25 (for low medium and high pressures) the results from the Aachen mechanism and the LLNL mechanism show excellent agreement with the experimental data at high temperatures and low temperatures. In the NTC region however, the results from the LLNL mechanism show slightly better agreement with the experimental data than the results from the Aachen mechanism. However, since the computation time for the LLNL mechanism is higher than the Aachen mechanism, we choose the latter for our calculation in this paper.

4.3 Simulated results

The conditions for the fuels were selected based on the request from a PhD student (Khristoffer) who performs experimental research into knock at Chalmers University.

We will now run Chemkin-Pro with the Aachen mechanism [32] to calculate the ignition delay times for a variety of fuel blends at various temperatures and pressures as stated below:

1. E10 (Lean, Stoichiometric and Rich conditions)
2. E10 (Lean conditions with EGR)
3. 95 unleaded (E5)
4. 98 unleaded (E5)

E10 stands for Gasoline with 10% ethanol and this widely used gasoline-ethanol blend has RON of 95. E10 is used all over the world for its environmental benefits and to increase the independence from major oil-producing countries.

4.3.1 RON 95 E10 (Lean, Stoichiometric and Rich conditions)

The simulations were carried out for the following conditions:

Conditions	Min	Max	Unit
Temperature (T)	600	1500	K
Pressure (P)	3	60	Bar
Equivalence ratio (ϕ)	0.4	1.4	1

All Ignition delay times are in seconds (s).

Fuel composition:

RON : 95 (10% ethanol by volume)
Iso-octane (mole%) : 63.8%
N-heptane (mole%) : 12.6%
Ethanol (mole%) : 23.6%

In Figures 26-31, The results of the simulations for three ϕ (lean stoichiometric and rich mixtures) values at three different pressures are reported.

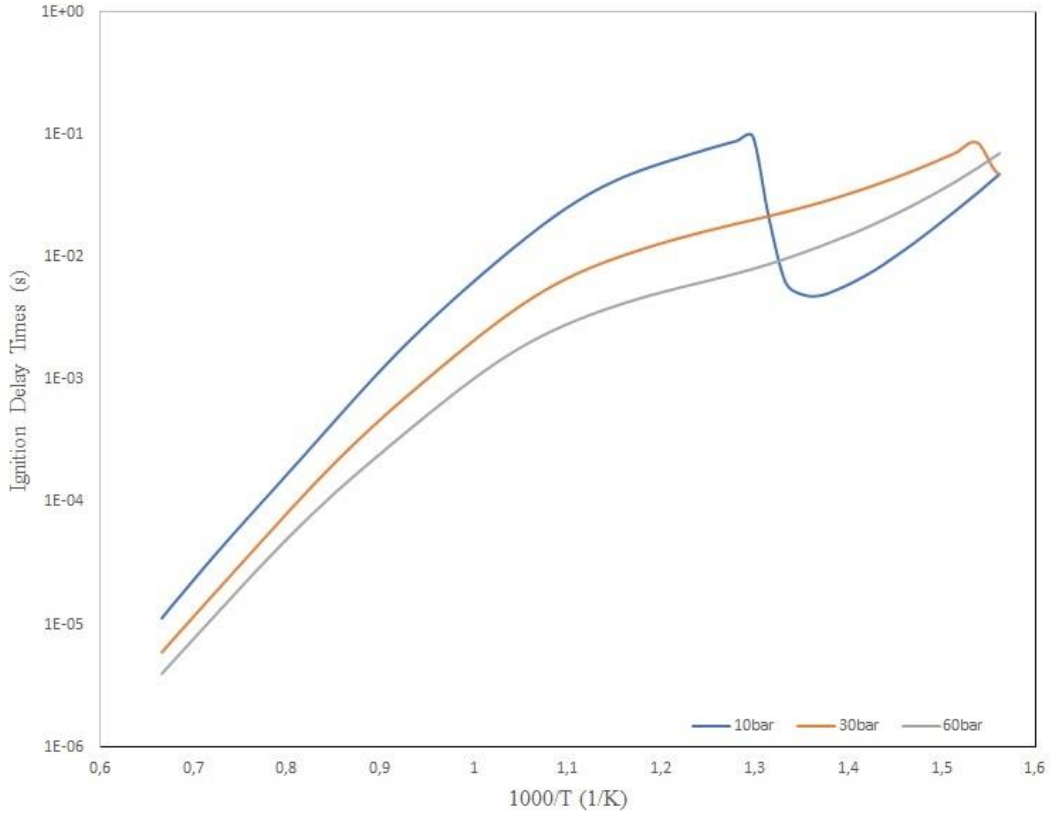

Figure 26: Ignition delay times calculated using the Aachen mechanism [32] for E10 at ϕ = 0.4; P = 10,30, 60bar.

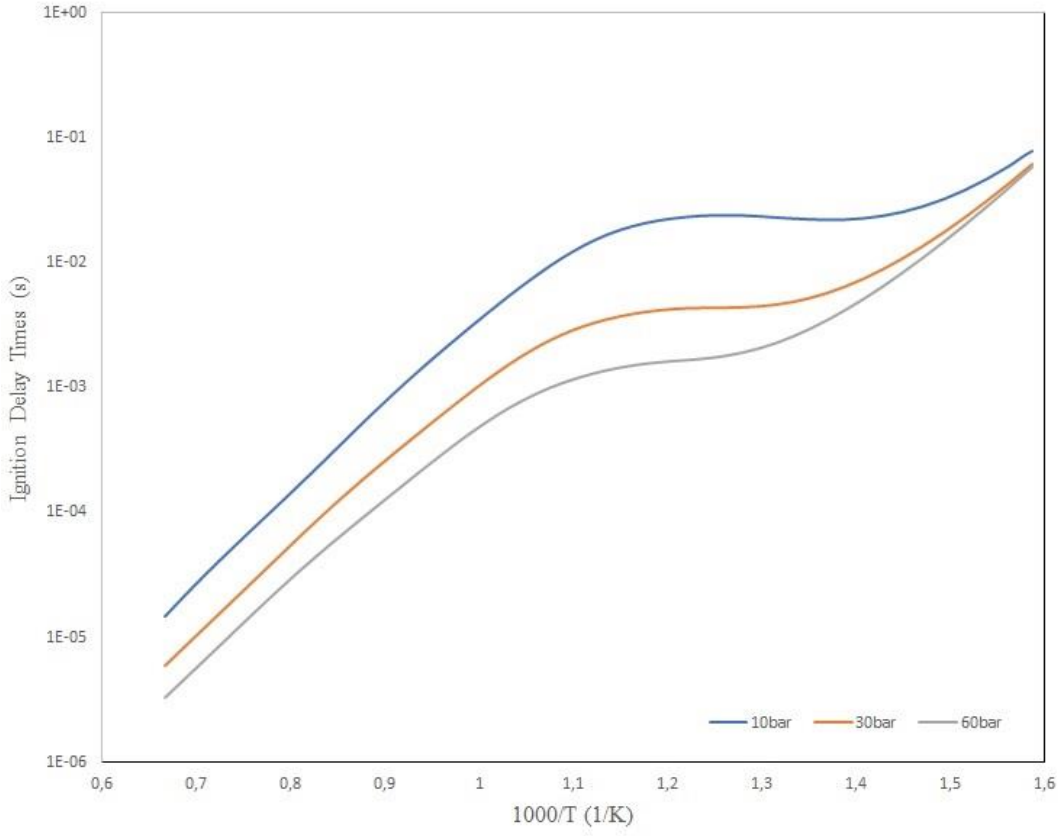

Figure 27: Ignition delay times calculated using the Aachen mechanism [32] for E10 at ϕ = 1; P = 10,30, 60bar.

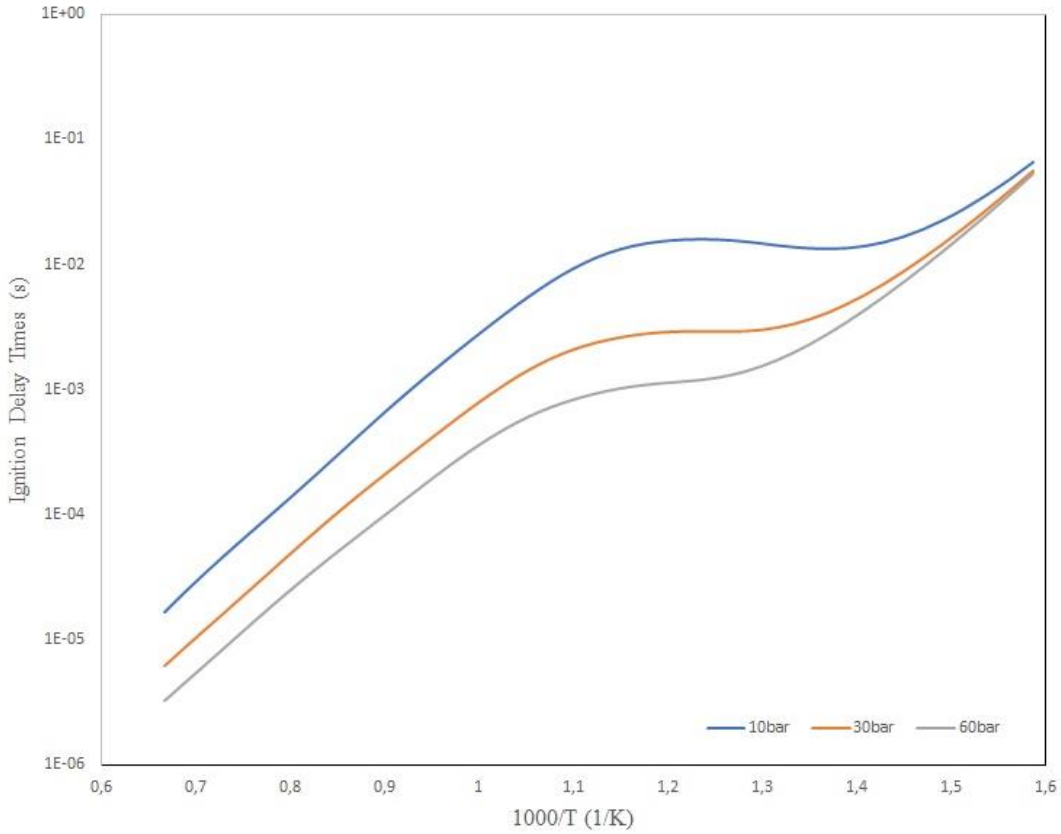

Figure 28: Ignition delay times calculated using the Aachen mechanism [32] for E10 at ϕ = 1.4; P = 10,30, 60bar.

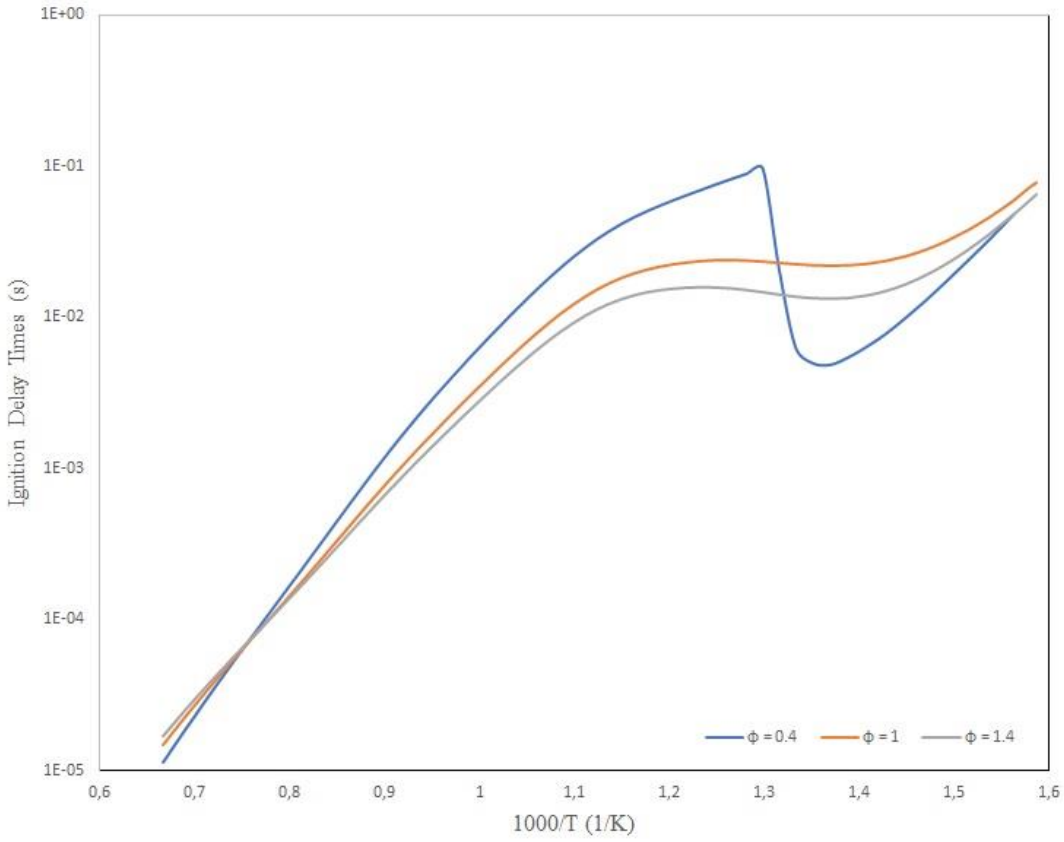

Figure 29: Ignition delay times calculated using the Aachen mechanism [32] for E10 at ϕ = 0.4, 1, 1.4; P = 10bar.

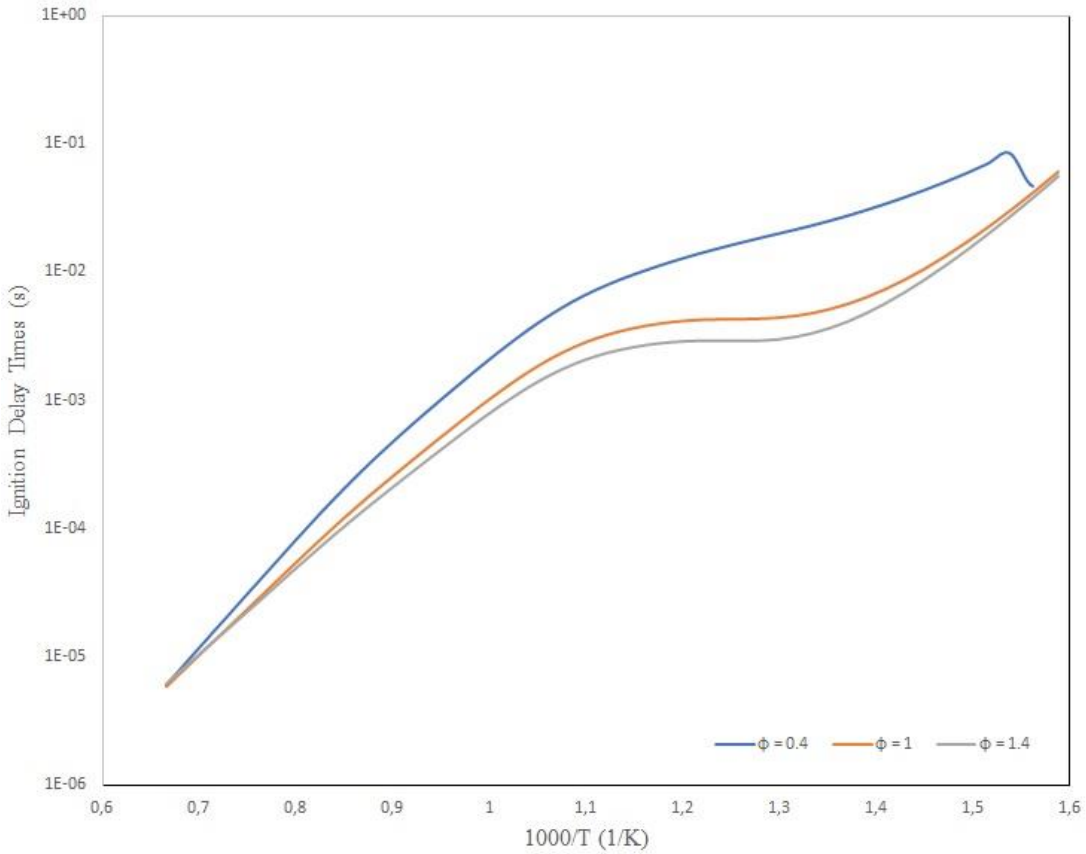

Figure 30: Ignition delay times calculated using the Aachen mechanism [32] for E10 at ϕ = 0.4, 1, 1.4; P = 30bar.

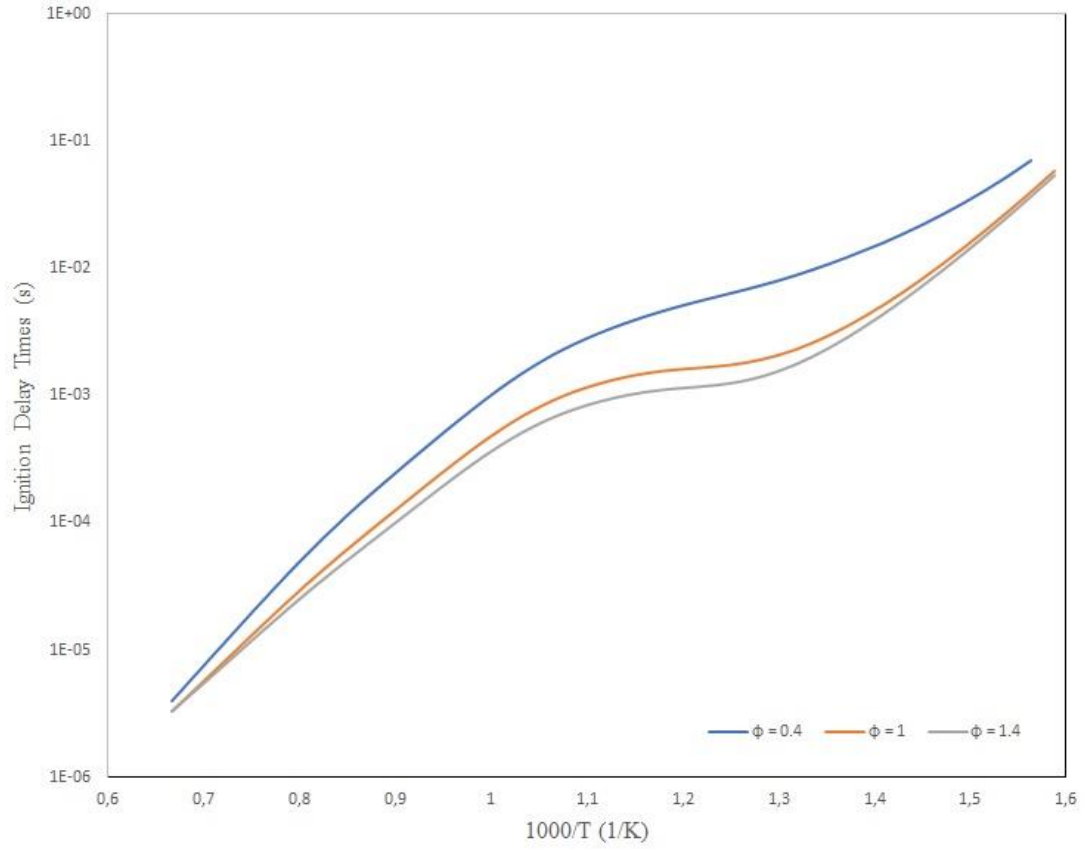

Figure 31: Ignition delay times calculated using the Aachen mechanism [32] for E10 at ϕ = 0.4, 1, 1.4; P = 60bar.

Figure 26 to 31 show the plots of ignition delay times vs inverse temperature for the equivalence ratio range of 0.4-1.4 and 10, 30 and 60bar pressures calculated using the Aachen mechanism [32].

4.3.1.1 Observed trends

Results reported in figures 26-31 show the following trends:

- In the Figures 26-28, we observe that the ignition delay times become shorter with increase in temperature except for the NTC region (intermediate temperature region) where the opposite is observed. The NTC region is not observed in lean mixtures.
- In Figure 26, at 10bar pressure, we notice an incoherent curve which dips down. This dip might me due to the chemical kinetic mechanism not being calibrated for a lean mixture at low pressure and temperature. This could also be due to the lean limit of the fuel/engine where the engine could misfire.
- In the Figures 26-28, we observe that the ignition delay times reduce with an increase in the pressure. We also observe that the NTC region becomes less pronounced as the pressure increases from 5bar to 40bar. Going even higher (60bar) flattens out the NTC region (in other words, the NTC region becomes less pronounced). The NTC region is also less pronounced at higher pressures. The authors in Ref. [8] attributed this trend to the increased stability of RO_2 radicals and faster decomposition of H_2O_2. In Figure 26., it is also seen that the pressure dependency in the NTC region is slightly lesser in lean mixtures compared stoichiometric mixtures.
- In Figures 28-31, it is observed that the effect ϕ is strongest in the intermediate temperature range i.e the NTC region. ϕ has very little effect in the high and low temperature regions. In Ref. [8], the authors attributed this trend to the important role of hydroperoxyl radical chemistry. It is also observed that the ignition delay times become shorter with increase in ϕ.

4.3.2 RON95 E10 (Lean conditions with EGR)

The simulations were carried out for the following conditions (conditions provided by the PhD student Kristoffer based on the experiments carried out by him at Chalmers University) and the main change as compared to the previous simulation is the addition of Exhaust Gas Recirculation (EGR). The minimum temperature limit was chosen as 650K as no ignition was observed below this temperature. The simulations were carried out for the following conditions.

Conditions	Min	Max	Unit
Temperature	650	750	K
Pressure	5	60	Bar
λ	1.4	2.5	1
Residuals/iEGR	0	10	% mass fraction

Exhaust gas composition:

λ	φ	CO2_WMFr (%)	CO_WMFr (%)	O2_WMFr (%)	N2_WMFr (%)	H2O_WMFr (%)	H2_WMFr (%)
1.4	0.71	15,06619	0,034139	5,792721	72,77591	5,997629	0,000683
1.8	0.56	11,2942	0,063953	10,22264	73,84124	4,513089	0,001284
2.5	0.4	12,40303	0,042433	8,988744	73,59375	4,943835	0,00085

All Ignition delay times are in seconds (s).

Fuel composition:

RON : 95 (10% ethanol by volume)
Iso-octane (mole%) : 63.8%
N-heptane (mole%) : 12.6%
Ethanol (mole%) : 23.6%

In Figures 32-46, The results of the simulations for three ϕ values at four different pressures and 3 different EGR rates are reported.

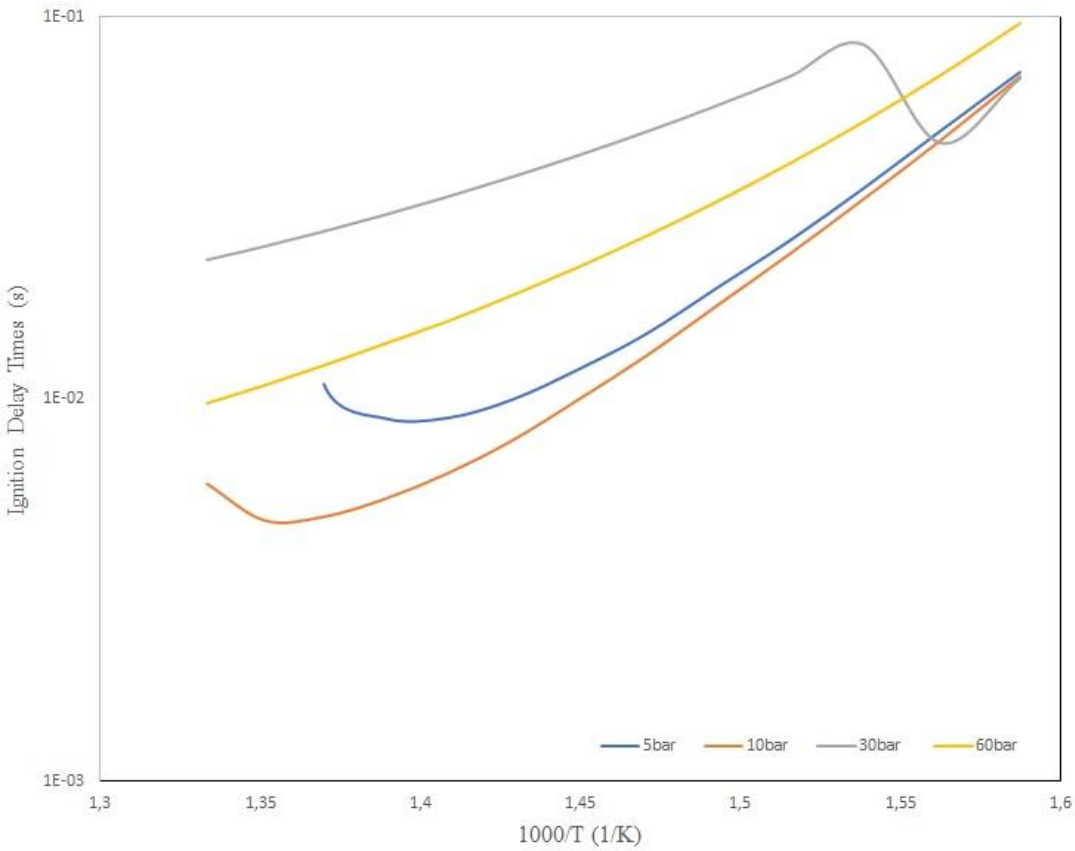

Figure 32: Ignition delay times calculated using the Aachen mechanism [32] for E10 at ϕ = 0.4; P = 5, 10, 30, and 60bar; EGR = 0%

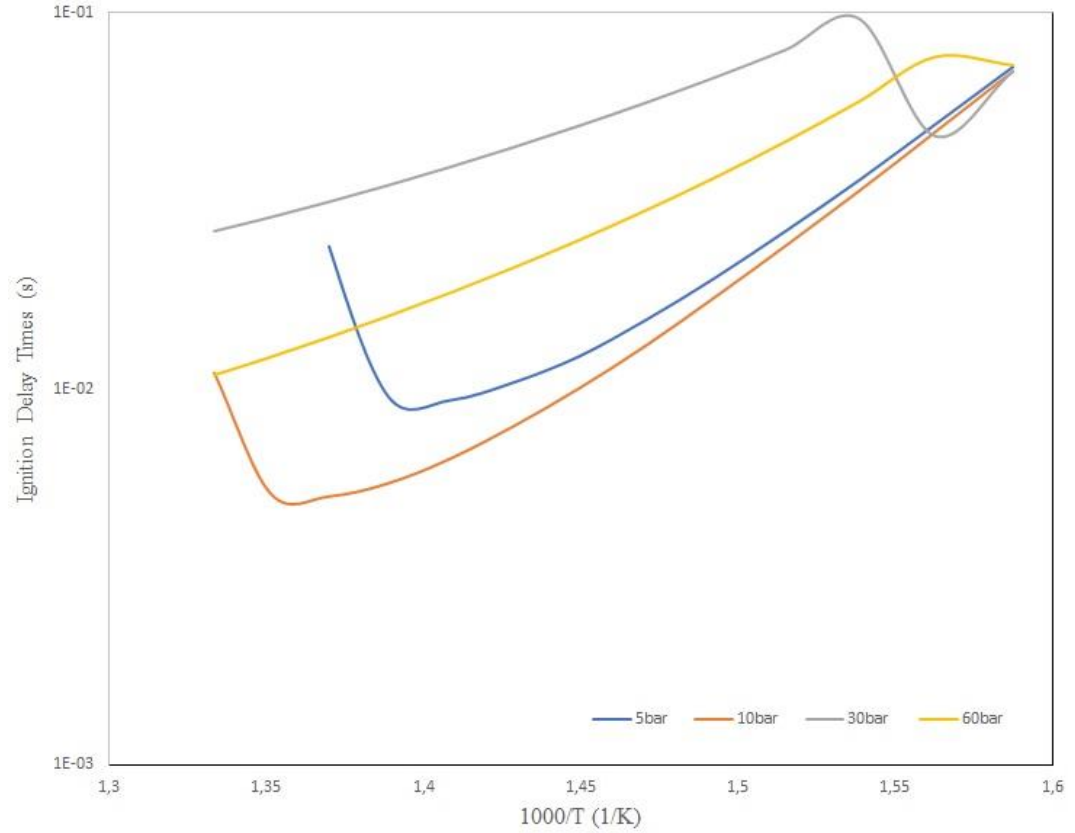

Figure 33: Ignition delay times calculated using the Aachen mechanism [32] for E10 at ϕ = 0.4; P = 5, 10, 30, and 60bar; EGR = 5%

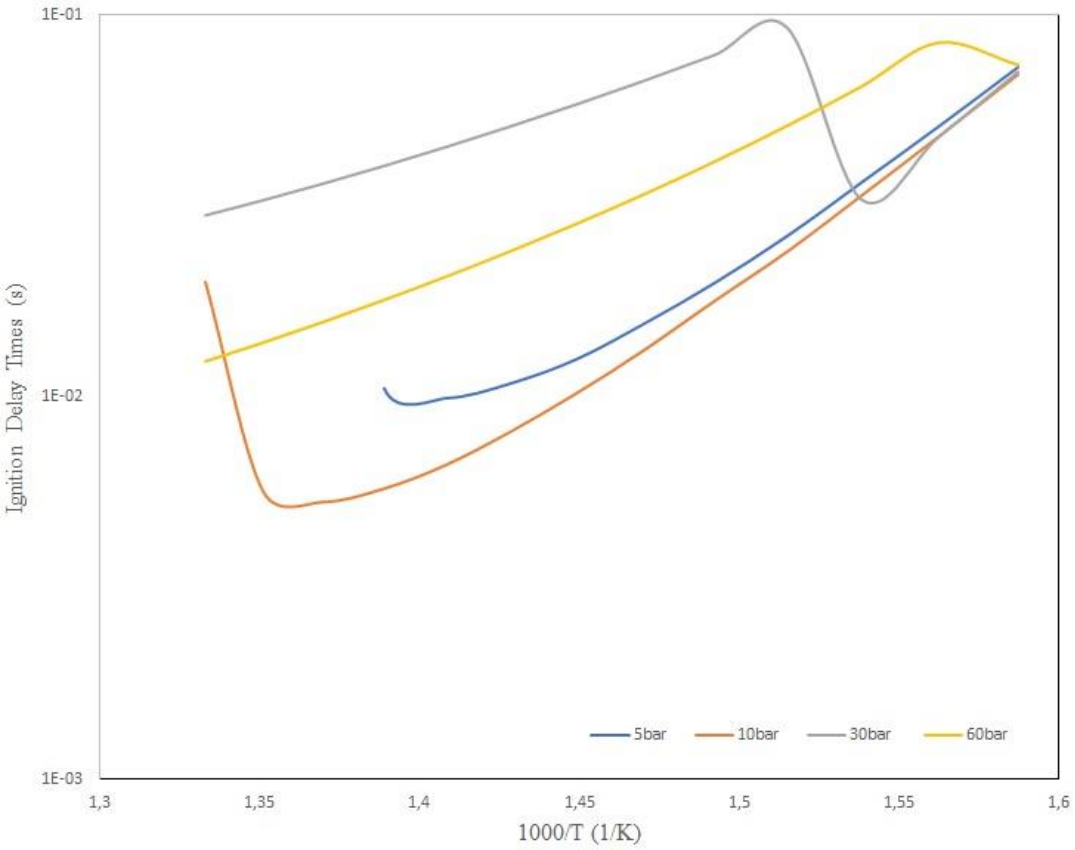

Figure 34: Ignition delay times calculated using the Aachen mechanism [32] for E10 at ϕ = 0.4; P = 5, 10, 30, and 60bar; EGR = 10%

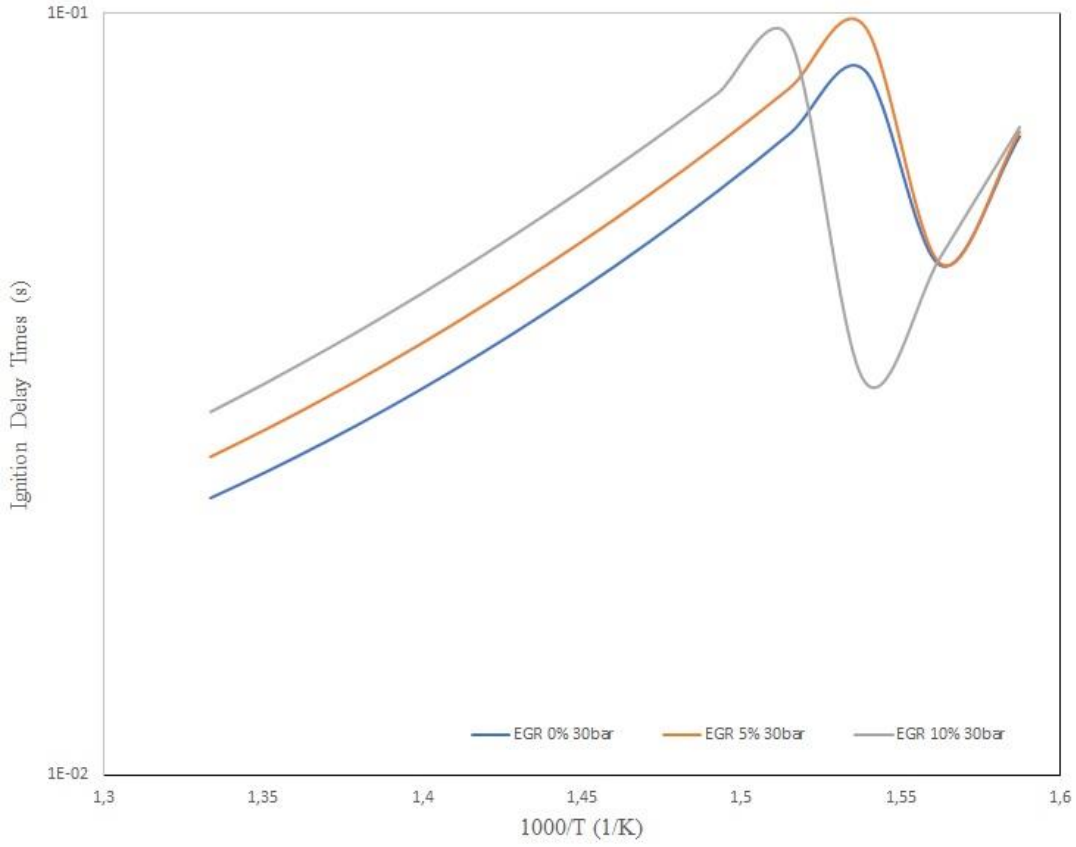

Figure 35: Ignition delay times calculated using the Aachen mechanism [32] for E10 at ϕ = 0.4; P = 30bar; EGR = 0%, 5% and 10%.

Figures 32-35 show the plots of ignition delay times vs inverse temperature at ϕ = 0.4 and for pressures of 5, 10, 30 and 60bar with EGR rates 0%, 5% and 10% calculated using the Aachen mechanism [32].

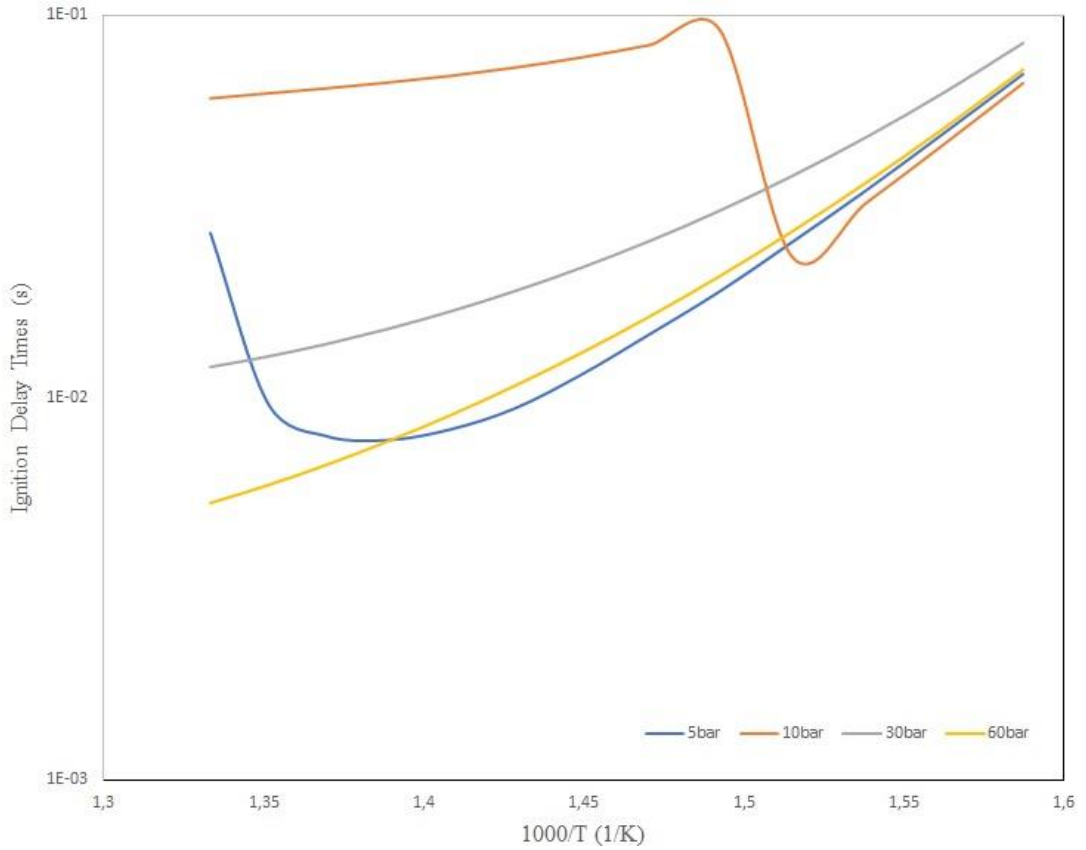

Figure 36: Ignition delay times calculated using the Aachen mechanism [32] for E10 at ϕ = 0.56; P =5, 10, 30, and 60bar; EGR = 0%.

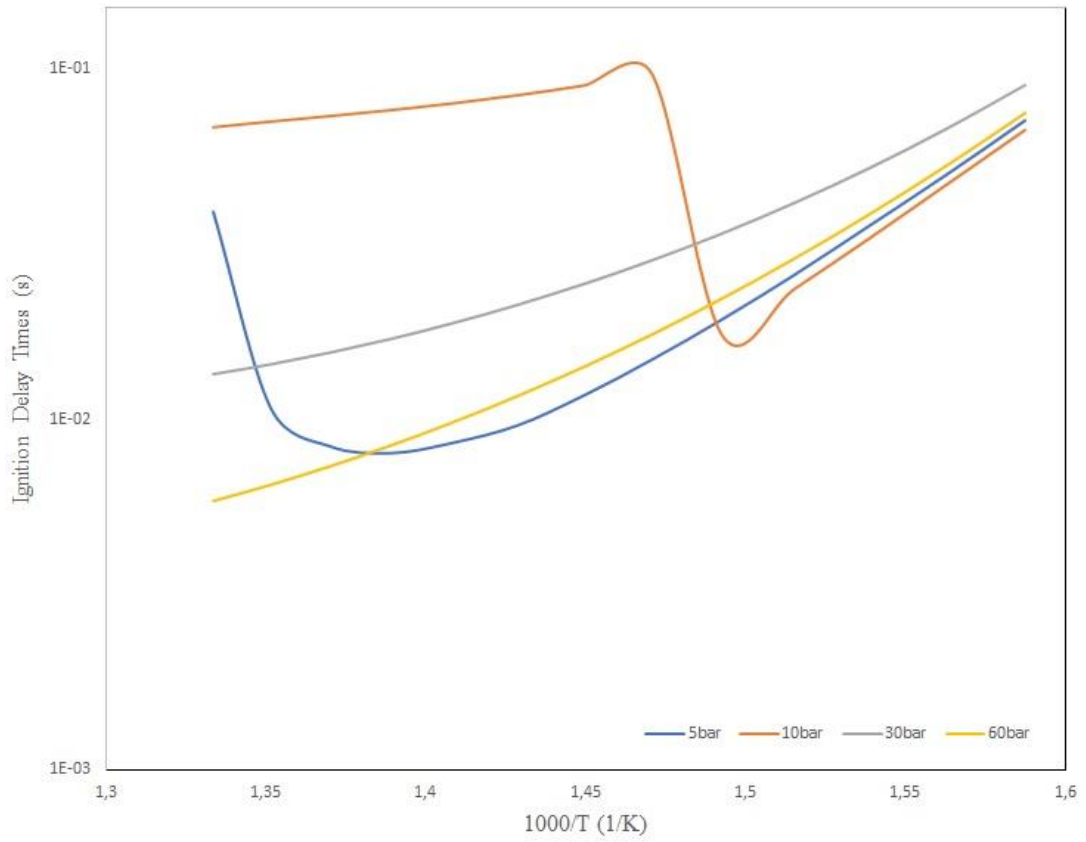

Figure 37: Ignition delay times calculated using the Aachen mechanism [32] for E10 at ϕ = 0.56; P =5, 10, 30, and 60bar; EGR = 5%.

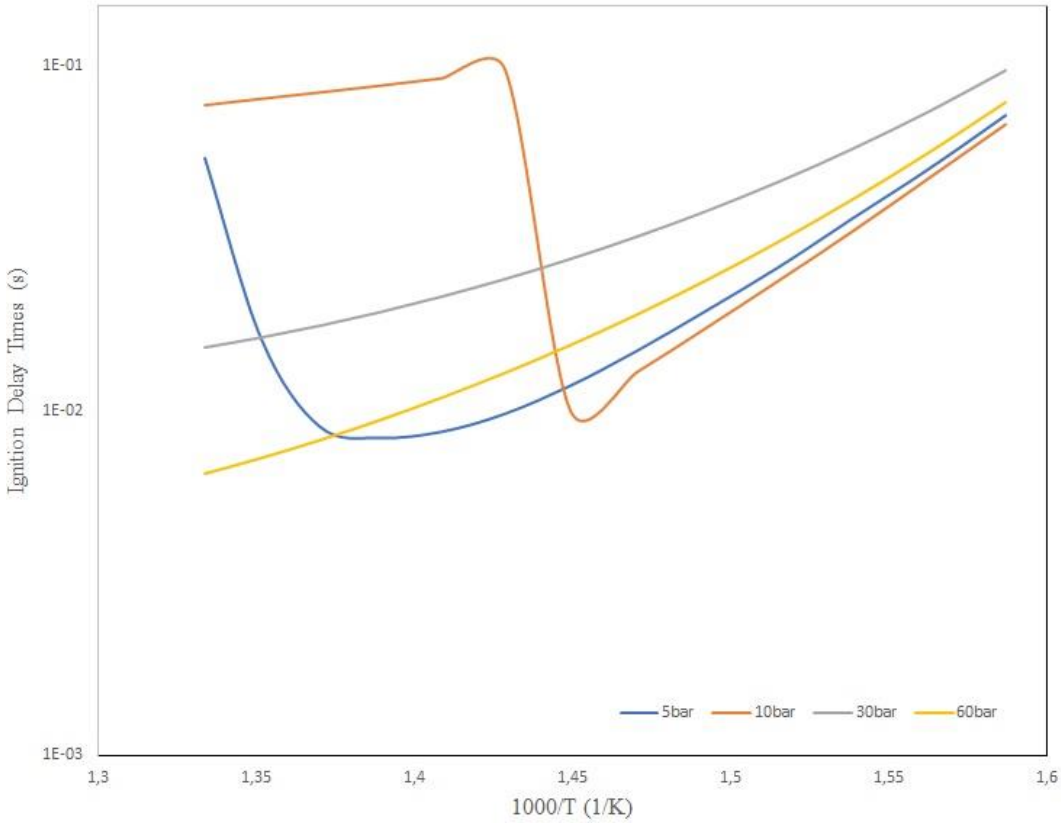

Figure 38: Ignition delay times calculated using the Aachen mechanism [32] for E10 at ϕ = 0.56; P =5, 10, 30, and 60bar; EGR = 10%.

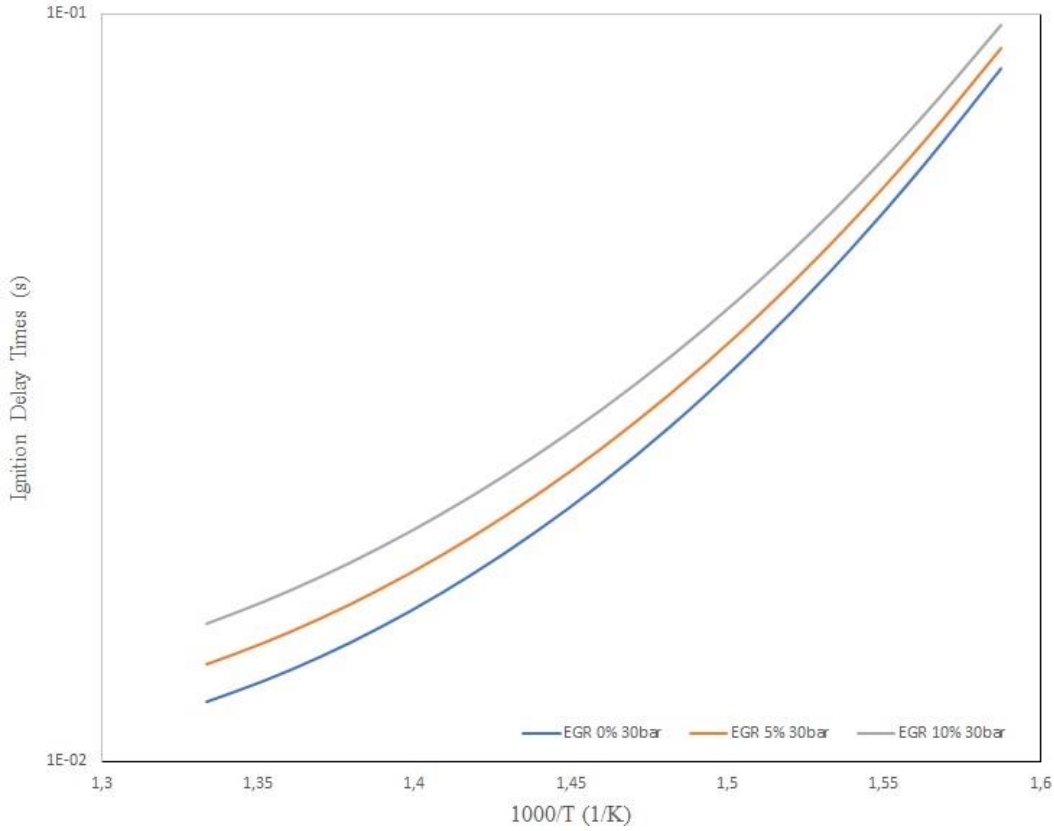

Figure 39: : Ignition delay times calculated using the Aachen mechanism [32] for E10 at ϕ = 0.56; P = 30bar; EGR = 0%, 5% and 10%.

Figures 36-39 show the plots of ignition delay times vs inverse temperature at ϕ = 0.56 and for pressures of 5, 10, 30 and 60bar with EGR rates 0%, 5% and 10% calculated using the Aachen mechanism [32].

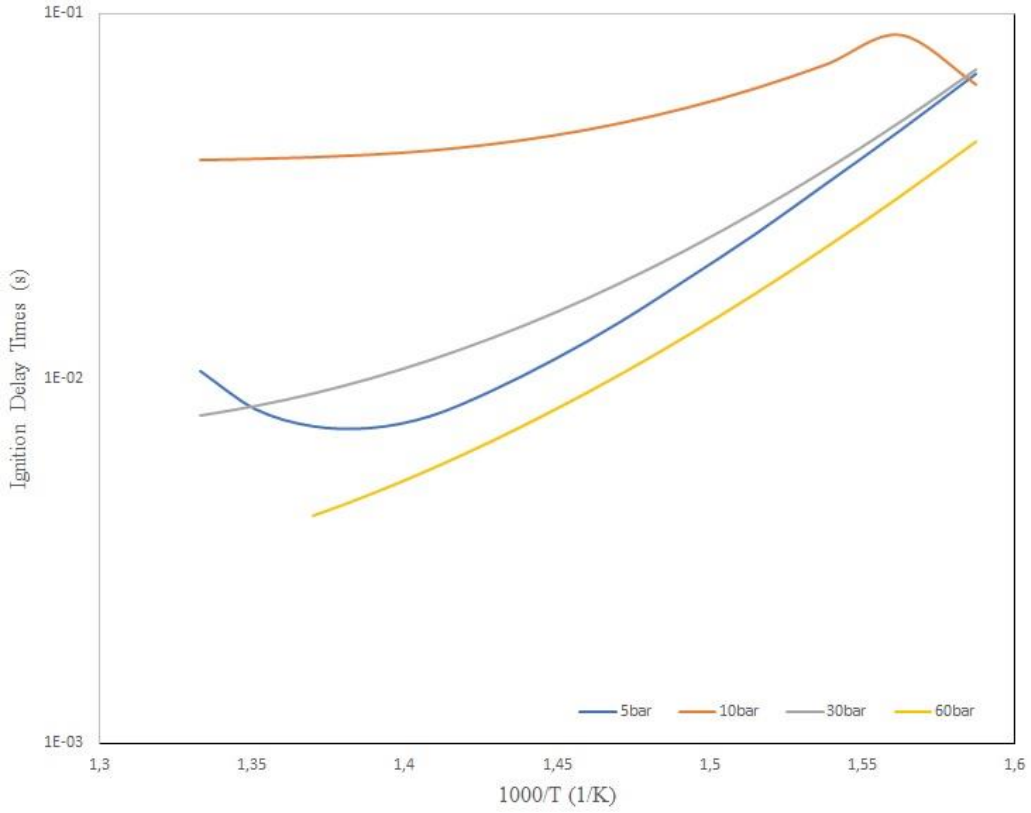

Figure 40: Ignition delay times calculated using the Aachen mechanism [32] for E10 at ϕ = 0.71; P =5, 10, 30, and 60bar; EGR = 0%.

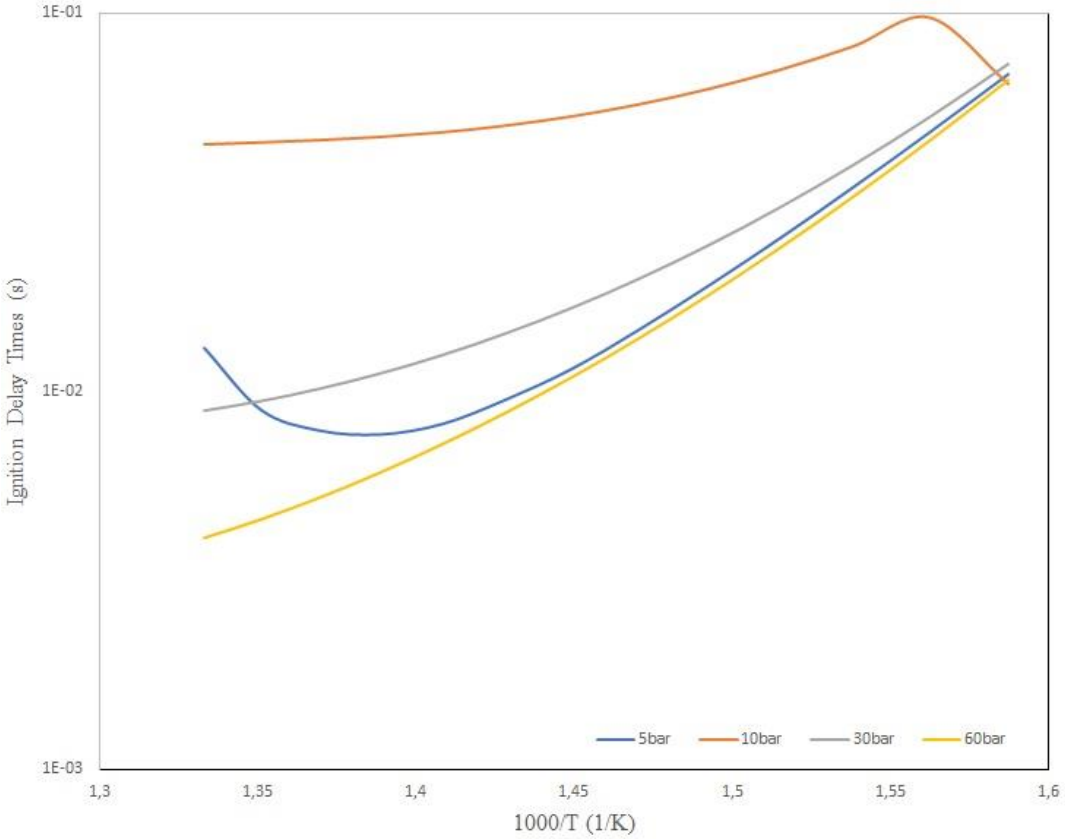

Figure 41: Ignition delay times calculated using the Aachen mechanism [32] for E10 at ϕ = 0.71; P =5, 10, 30, and 60bar; EGR = 5%.

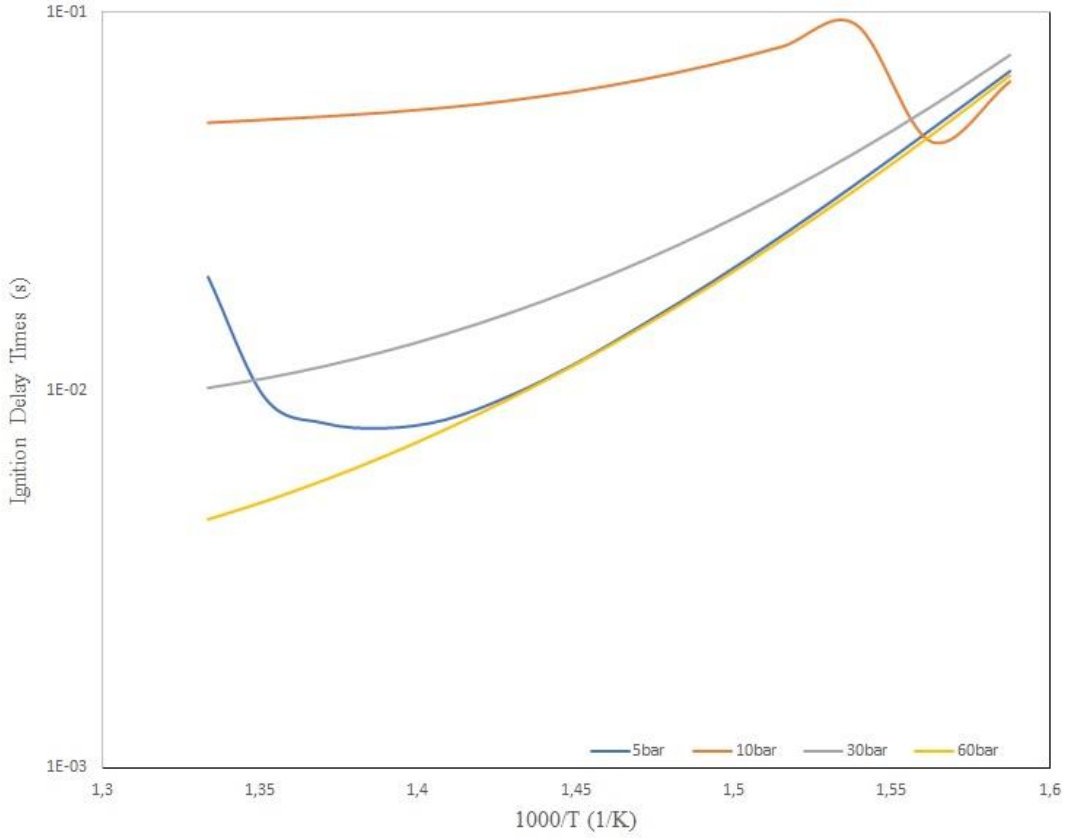

Figure 42: Ignition delay times calculated using the Aachen mechanism [32] for E10 at ϕ = 0.71; P =5, 10, 30, and 60bar; EGR = 10%.

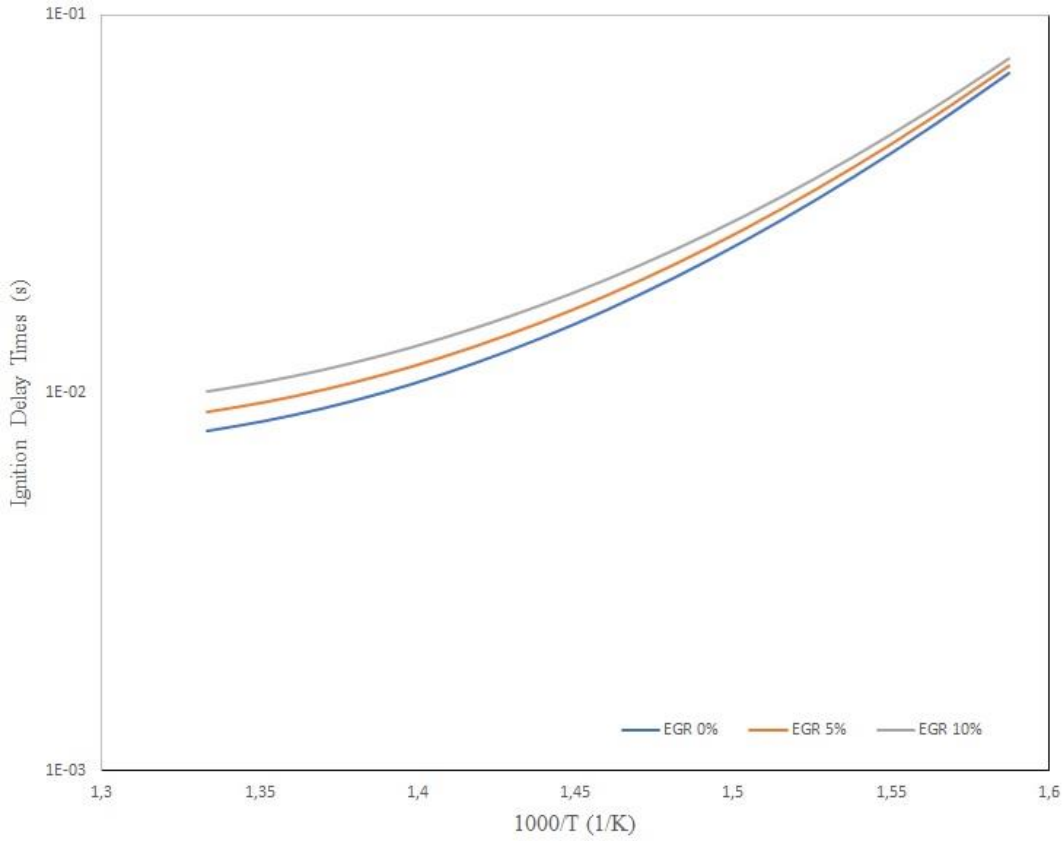

Figure 43: : Ignition delay times calculated using the Aachen mechanism [32] for E10 at ϕ = 0.71; P = 30bar; EGR = 0%, 5% and 10%.

Figures 40-43 show the plots of ignition delay times vs inverse temperature at ϕ = 0.71 and for pressures of 5, 10, 30 and 60bar with EGR rates 0%, 5% and 10% calculated using the Aachen mechanism [32].

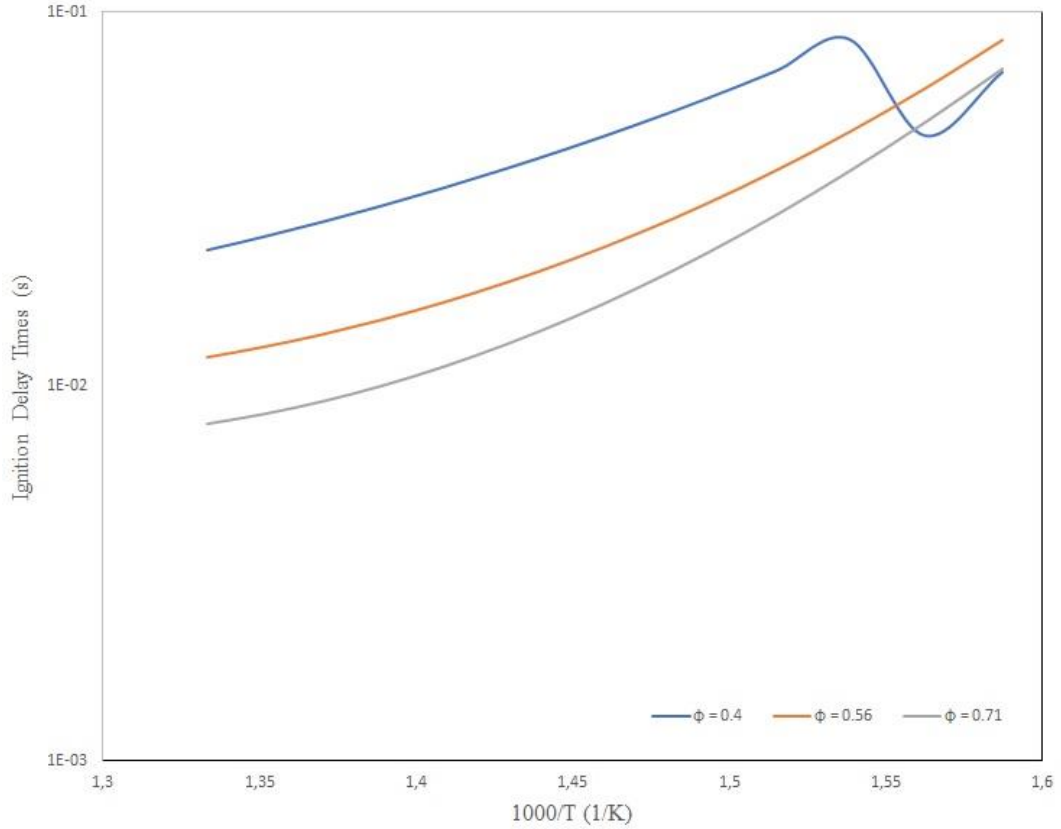

Figure 44: Ignition delay times calculated using the Aachen mechanism [32] for E10 at ϕ = 0.4, 0.56, and 0.71; P = 30bar; EGR = 0%.

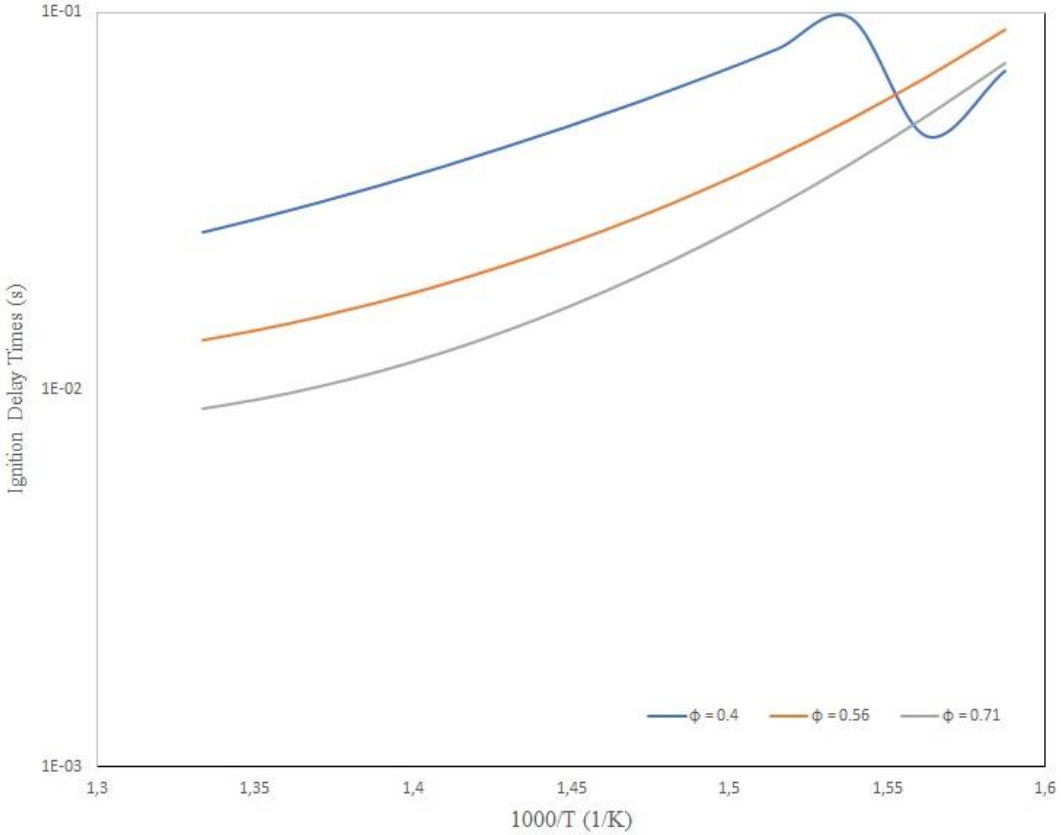

Figure 45: Ignition delay times calculated using the Aachen mechanism [32] for E10 at ϕ = 0.4, 0.56, and 0.71; P = 30bar; EGR = 5%.

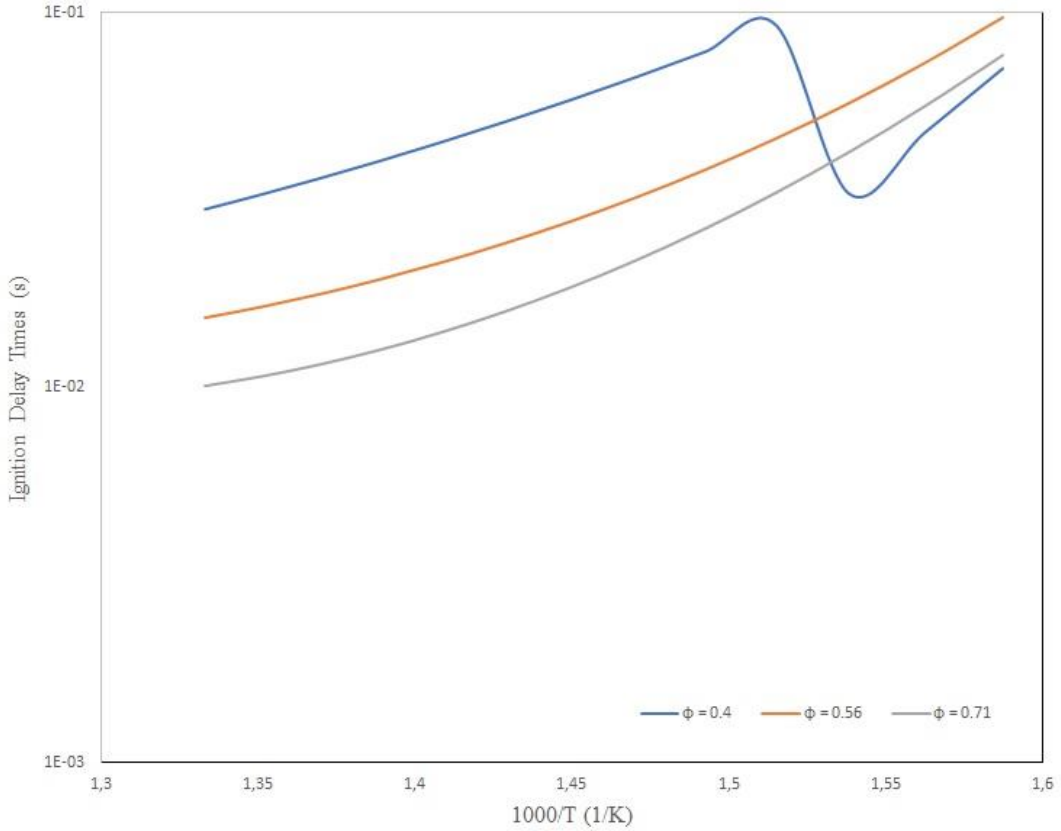

Figure 46: Ignition delay times calculated using the Aachen mechanism [32] for E10 at ϕ = 0.4, 0.56, and 0.71; P = 30bar; EGR = 10%.

Figures 44-46 show the dependence of Ignition delay times at EGR rates of 0%, 5% and 10% and how they vary at three ϕ values. Ignition delay times are calculated using the Aachen mechanism [32].

4.3.2.1 Observed trends

- As this simulation is for the same fuel as in the previous section, all the observed trends are similar to the trends discussed in Section 4.3.1.1.
- In Figures 32 - 46, we observe that the ignition delay times reduce with an increase in the pressure and temperature.
- In Figures 32 – 34, at pressures below 10bar, we notice an incoherent curve which dips down. This dip might me due to the chemical kinetic mechanism not being calibrated for a lean mixture at low pressure and temperature. This could also be due to the lean limit of the fuel/engine where the engine could misfire. As ϕ increases, this irregularity reduces and cannot be observed at 10bar but is still present at 5bar (Figure 40).
- In Figure 44., we observe that the Ignition delay times become shorter with increase in ϕ.
- Comparing Figure 35., 39., and 43., we observe that as the EGR rate increases, the ignition delay times increase. Hence better knock resistance
- Comparing Figure 44., 45., and 46., The effect of EGR is consistent at all 3 ϕ values.

4.3.3 95 Unleaded (E5)

The simulations were carried out for 95 (RON 95) unleaded petrol:

Conditions	Min	Max	Unit
Temperature (T)	650	1400	K
Pressure (P)	3	80	Bar
Equivalence ratio (ϕ)	0.4	1.6	1

Fuel composition:

RON : 95 (5% ethanol by volume)
Iso-octane (mole%) : 78.5%
N-heptane (mole%) : 8.7%
Ethanol (mole%) : 12.8%

In Figure 47., The results of the simulation of 95 Unleaded petrol at ϕ = 1 and Pressures of 5, 10, 40, and 80bar are reported.

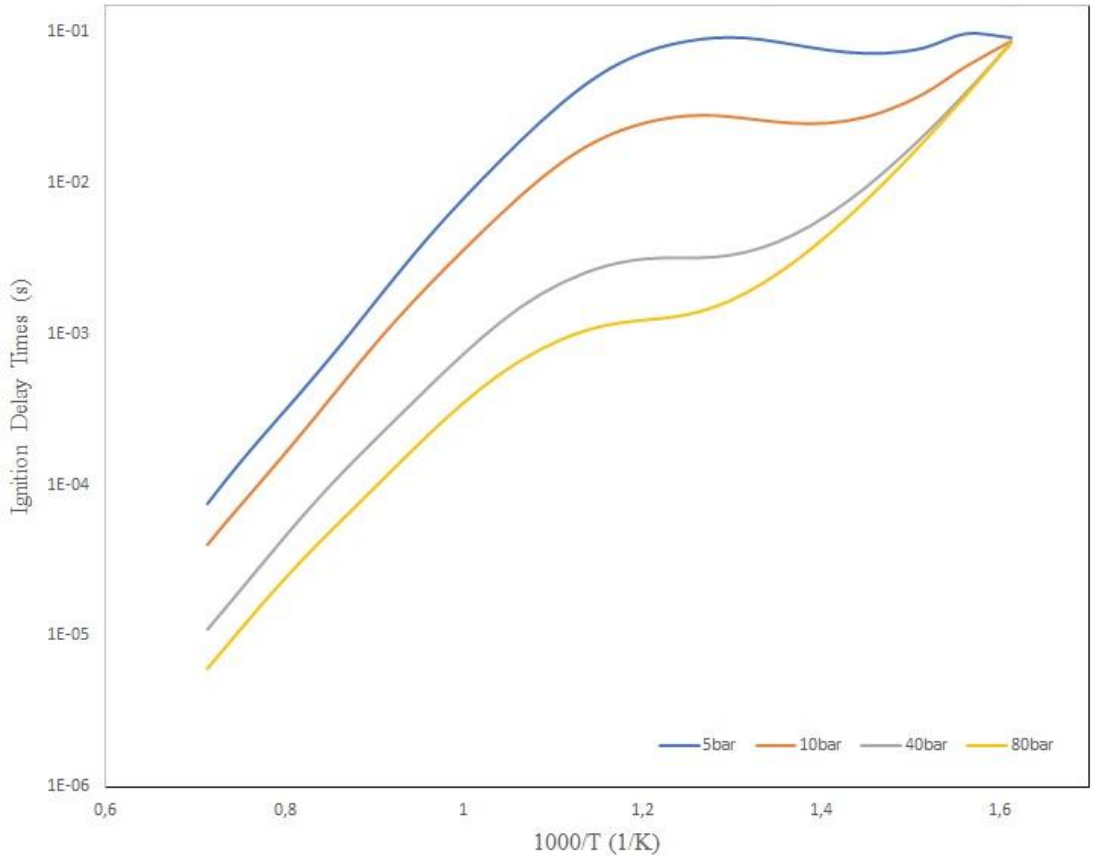

Figure 47: Ignition delay times calculated using the Aachen mechanism [32] for 95 Unleaded at ϕ = 1; P = 5, 10, 40, and 80bar.

4.3.3.1 Observed trends:

- As this simulation is for a fuel of RON95, all the observed trends are similar to the trends discussed in Section 4.3.1.1.
- Ignition delay times increase with increase in pressure and ϕ. The ignition delay times increase with an increase in temperature except in the NTC region.
- No new trend is observed as compared to Section 4.3.1.1.

4.3.4 98 Unleaded (E5)

The simulations were carried out for 98 (RON 98) unleaded petrol:

Conditions	Min	Max	Unit
Temperature (T)	650	1400	K
Pressure (P)	3	80	Bar
Equivalence ratio (ϕ)	0.4	1.6	1

Fuel composition:

RON : 98 (5% ethanol by volume)
Iso-octane (mole%) : 81.3%
N-heptane (mole%) : 5.8%
Ethanol (mole%) : 12.9%

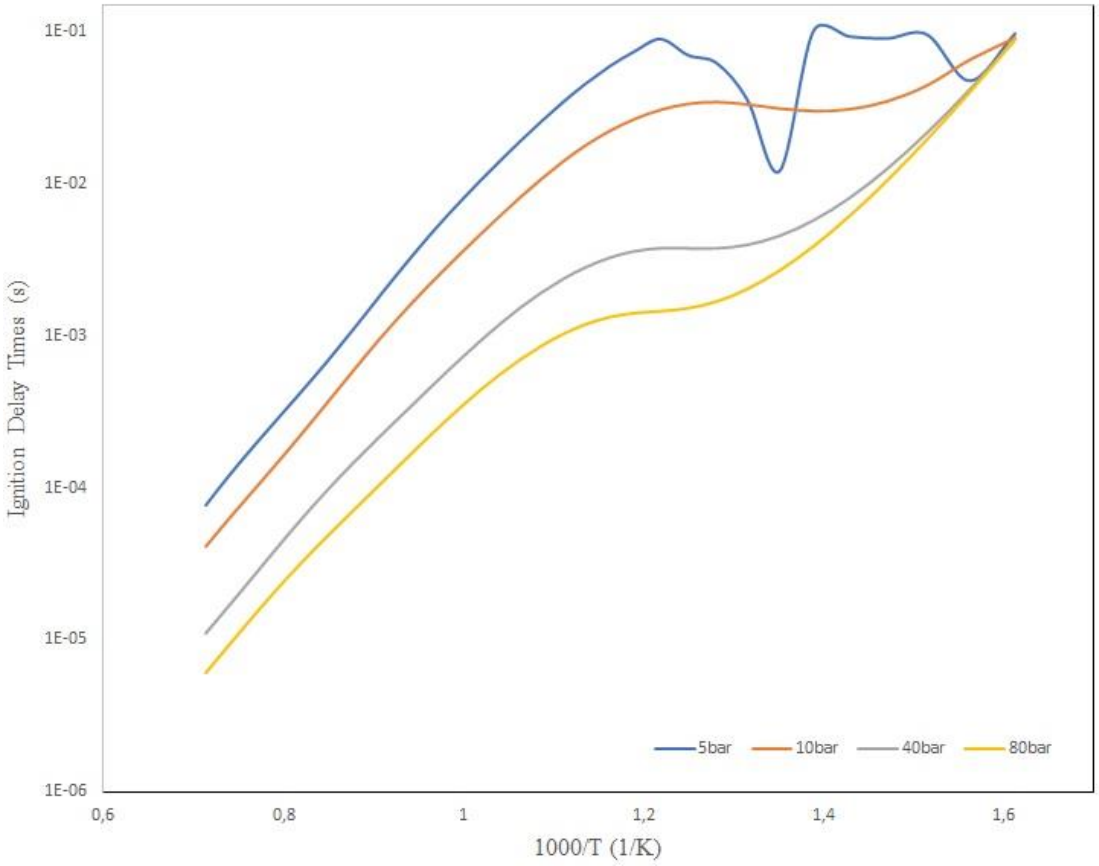

Figure 48: Ignition delay times calculated using the Aachen mechanism [32] for 95 Unleaded at ϕ = 1; P = 5, 10, 40, and 80bar.

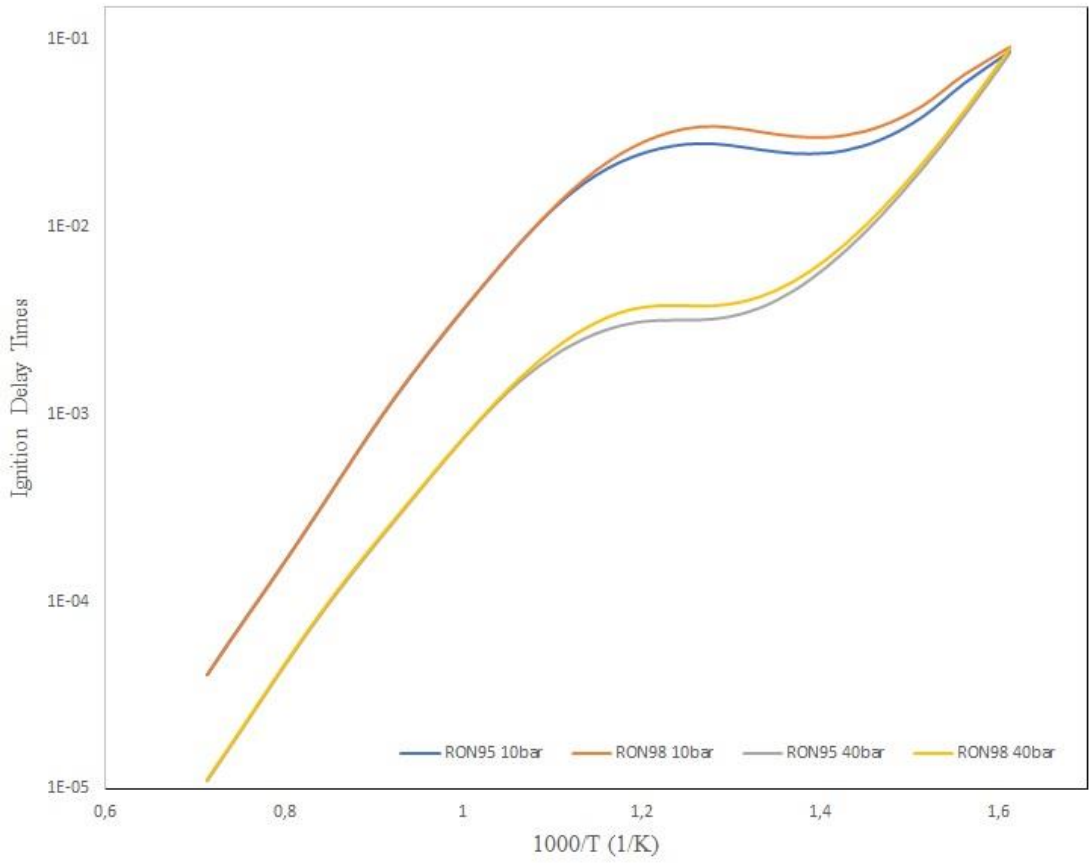

Figure 49: Comparison between Ignition delay times calculated using the Aachen mechanism [32] for 95Unleaded and 98 Unleaded at ϕ = 1, P = 10 and, 40 bar.

4.3.4.1 Observed trends

- As this simulation is for a fuel of RON98, all the observed trends are similar to the trends discussed in Section 4.3.1.1 as the fuel composition is similar.
- Ignition delay times increase with increase in pressure and ϕ. The ignition delay times increase with an increase in temperature except in the NTC region.
- In Figure 49., It can be observed that the ignition delay times are almost independent of composition in the high-temperature and low-temperature regions. However, the fuel composition does have an appreciable effect at intermediate temperatures. It is observed that the ignition delay times are lower for RON 98 in the NTC region as compared to RON 95 and this result can be observed at 10 and 40bar pressures. Increasing the iso-octane fraction (PRF 95 to PRF 98) results in longer ignition delay times hence increasing resistance to knocking.

4.3.5 Best operating range:

The simulations carried out in our thesis were for set parameters and the actual ignition in an engine was not simulated. A criterion was chosen in order to suggest the best operating range of an engine to mitigate knock. Based on the experimental data from Ref. [7], for a high-torque and high-load scenario in an engine (knock prone region), knock was observed for ignition delay times longer than 0.5ms (the details of the study are discussed in detail in section 2.5) and this criterion was chosen to suggest the best operating range to mitigate knock.

4.3.5.1 RON 95 E10 (General conditions)

Pressure	ϕ = 0.4	ϕ = 0.6	ϕ = 0.8	ϕ = 1	ϕ = 1.2	ϕ = 1.4
03 bar	T<1230K	T<1230K	T<1230K	T<1230K	T<1230K	T<1230K
05 bar	T<1200K	T<1200K	T<1195K	T<1190K	T<1190K	T<1190K
10 bar	T<1170K	T<1160K	T<1150K	T<1145K	T<1140K	T<1135K
15 bar	T<1150K	T<1135K	T<1120K	T<1115K	T<1105K	T<1100K
20 bar	T<1130K	T<1110K	T<1100K	T<1090K	T<1080K	T<1075K
25 bar	T<1120K	T<1100K	T<1080K	T<1070K	T<1060K	T<1050K
30 bar	T<1115K	T<1085K	T<1070K	T<1055K	T<1045K	T<1035K
35 bar	T<1095K	T<1070K	T<1055K	T<1040K	T<1030K	T<1020K
40 bar	T<1085K	T<1060K	T<1045K	T<1030K	T<1020K	T<1010K
45 bar	T<1075K	T<1050K	T<1035K	T<1020K	T<1010K	T<1000K
50 bar	T<1070K	T<1045K	T<1025K	T<1010K	T<1000K	T<990K
55 bar	T<1060K	T<1035K	T<1020K	T<1005K	T<990K	T<980K
60 bar	T<1055K	T<1030K	T<1010K	T<995K	T<980K	T<970K

Table 3: Best operating range to avoid knock for E10 at various temperatures and pressures.

4.3.5.2 RON 95 E10 (Chalmers conditions)

The ignition delay time threshold is selected from the validation as discussed in section 3.

In this simulation, the operating temperature range is 650K to 750K. The main aim of this simulation was to study the effect of EGR on lean mixtures. The least ignition delay time in this simulation is higher than 5ms (which is our chosen criteria for knock prediction) as observed in the all the above graphs (Figures 32 - 46). It can be concluded that there is no knock observed in this operating range for RON 95 E10.

4.3.5.3 95 Unleaded (E5)

Pressure	ϕ = 0.4	ϕ = 0.6	ϕ = 0.8	ϕ = 1	ϕ = 1.2	ϕ = 1.4	ϕ = 1.6
03 bar	T<1235K	T<1240K	T<1240K	T<1250K	T<1250K	T<1260K	T<1260K
05 bar	T<1210K	T<1200K	T<1200K	T<1200K	T<1200K	T<1200K	T<1200K
10 bar	T<1170K	T<1160K	T<1150K	T<1150K	T<1150K	T<1140K	T<1140K
20 bar	T<1130K	T<1120K	T<1110K	T<1090K	T<1080K	T<1075K	T<1070K
40 bar	T<1090K	T<1060K	T<1040K	T<1030K	T<1020K	T<1010K	T<1000K
60 bar	T<1050K	T<1030K	T<1010K	T<1000K	T<980K	T<970K	T<960K
80 bar	T<1030K	T<1010K	T<990K	T<970K	T<950K	T<940K	T<920K

Table 4:Best operating range to avoid knock for 95 Unleaded (E5) at various temperatures and pressures.

4.3.5.4 98 Unleaded (E5)

Pressure	ϕ = 0.4	ϕ = 0.6	ϕ = 0.8	ϕ = 1	ϕ = 1.2	ϕ = 1.4	ϕ = 1.6
03 bar	T<1230K	T<1240K	T<1240K	T<1250K	T<1260K	T<1260K	T<1260K
05 bar	T<1205K	T<1205K	T<1205K	T<1205K	T<1200K	T<1200K	T<1200K
10 bar	T<1175K	T<1160K	T<1155K	T<1155K	T<1150K	T<1140K	T<1140K
20 bar	T<1135K	T<1120K	T<1110K	T<1095K	T<1095K	T<1080K	T<1070K

40 bar	T<1090K	T<1060K	T<1045K	T<1035K	T<1020K	T<1015K	T<1000K
60 bar	T<1055K	T<1035K	T<1015K	T<1000K	T<985K	T<970K	T<960K
80 bar	T<1035K	T<1010K	T<990K	T<970K	T<955K	T<940K	T<930K

Table 5: Best operating range to avoid knock for 98 Unleaded (E5) at various temperatures and pressures.

5 Conclusion

In the present work a numerical study was performed on the commercially available fuels to study their ignition delay times and understand the best operating range of the fuels in an SI engine.

Three chemical kinetic mechanisms from Aachen university [32], KAUST [37], and LLNL [39] were validated and the results computed from these mechanisms are shown in section 4.1. The mechanism from Aachen university was chosen as it has the least error percentage when compared to the experimental results. Using the Aachen mechanism [32], ignition delay times were calculated for three different fuel blends at lean, stoichiometric and rich conditions for a temperature range between 600K to 1500K and a pressure range between 5bar to 60bar. For the simulation in section 4.3.2 EGR range of 0% to 10% were also studied.

Results show the following trends:

- Increase in pressure leads to shorted ignition delay times when the other parameters remain constant. Ignition delay times in the NTC region exhibit a lower dependency on pressure for lean mixtures.
- Increase in ϕ leads to shorter ignition delay times (when the other parameters remain constant) and a high dependency on ϕ in the NTC region is observed and the opposite in the high and low temperature regions.
- The knock resistance of a fuel increases with increase in the RON of a fuel. However, the fuel composition plays a negligible role in the high and low temperature regions and the effect is mostly noticed in the NTC region.
- Higher temperature leads to a shorter ignition delay time. However, the opposite is true in the NTC region.

All the above observed trends are consistent with the theoretical and numerical results in Ref. [3] and Ref. [8].

Knock mitigation strategies:

- EGR is the second most applied strategy. Cool EGR has more potential in knock mitigation without the loss of output power.
- RON – using a fuel of higher RON can help mitigate knock but this requires an engine which can run on fuels of different RON.
- Cooling of the combustion chamber walls is also an effective approach to reduce end-gas temperatures (lower input temperature leads to lower ignition delay times).

6 Future Work:

- The influence of the fuel composition can be studied further by calculating and comparing the ignition delay times for fuels blends with varying RON values.
- Different fuel surrogates can be tested for the same input conditions.
- Different EGR and Ethanol percentage can be studied for the same input conditions.

7 References

[1] Heywood, J. B. (1988): *Internal combustion engine fundamentals*. McGraw-Hill Inc., United States of America.

[2] Stone, R. (2012): *Introduction to Internal combustion engines*. Macmillan, United Kingdom

[3] Wang, Z., Liu, H., Reitz, R. D. (2017): Knocking combustion in spark-ignition engines. *Progress in Energy and Combustion Science*, Vol. 61, July 2017, pp. 78–112.

[4] ASTM D2699-19 (2019): *Standard Test Method for Research Octane Number of Spark-Ignition Engine Fuel*, ASTM International, West Conshohocken, PA, 2019, www.astm.org.

[5] ASTM D2700-19 (2019): *Standard Test Method for Motor Octane Number of Spark-Ignition Engine Fuel*, ASTM International, West Conshohocken, PA, 2019, www.astm.org.

[6] Kalghatgi, T. G. (2005): Auto-ignition quality of practical fuels and implications for fuel requirements of future SI and HCCI engines. *SAE Technical Paper 2005-01-0239*, 2005.

[7] Kalghatgi, T. G. (2016:) Knock Prediction using a Simple Model for Ignition Delay. *SAE Technical Paper 2016-01-0702*, 2016.

[8] AlAbbad, M., Javed, T., Khaled, F., Badra, J., Farooq, A. (2017): Ignition delay time measurements of primary reference fuel blends. *Combustion and Flame*, Vol. 178, April 2017, pp. 205–216.

[9] Çengel, Y., Boles, M. (2008): *Thermodynamics – An Engineering Approach*. McGraw-Hill Higher Education, Boston.

[10] Ciezki, H. K., Adomeit, G. (1993): Shock-tube investigation of self-ignition of n-heptane-air mixtures under engine relevant conditions. *Combustion and Flame*, Vol. 93, No. 4, June 1993, pp. 421-433.

[11] Naidja, A., Krishna, C. R., Butcher, T., Mahajan, D. (2003): Cool flame partial oxidation and its role in combustion and reforming of fuels for fuel cell systems. *Progress in Energy and Combustion Science*, Vol. 29, No. 2, 2003, pp. 155-191.

[12] Law, C. K., Zhao, P. (2012): NTC-affected ignition in nonpremixed counterflow. *Combustion and Flame*, Vol. 159, No. 3, March 2012, pp. 1044-10540

[13] Livengood, J. C., Wu, P. C. (1995): Correlation of autoignition phenomena in internal combustion engines and rapid compression machines. *Symposium (International) on combustion*, Vol. 5, No. 1, 1995, pp. 347-356.

[14] Kalghatgi, T. G., Nakata, K., Mogi, K. (2005): Octane appetite studies in direct injection spark ignition (DISI) engines. *SAE Technical Paper 2005-01-0244*, 2005.

[15] Kalghatgi, T. G., Risberg, P., Ångstrom H-E. (2003): A method of defining ignition quality of fuels in HCCI engines. *SAE Technical Paper 2003-01-1816*, 2003.

[16] Risberg, P., Kalghatgi, T. G., Ångstrom, H-E. (2003): Auto-ignition quality of gasoline-like fuels in HCCI engines. *SAE Technical Paper 2003-01-3215*, 2003.

[17] Kalghatgi, T. G., Head, R. A. (2004): The available and required autoignition quality of gasoline - like fuels in HCCI engines at high temperatures. *SAE Technical Paper 2004-01-1969*, 2004.

[18] Curran, H. J., Pitz, W. J., Westbrook, C. K., Callahan, G. V., Dryer, F. L. (1998): Oxidation of automotive primary reference fuels at elevated pressures. *Symposium (International) on combustion*, Vol. 27, No. 2, 1998, pp. 379-387.
[19] Zhang, P., Ji, W., He, T., He, X., Wang, Z., Yang, B., Law, C. K. (2016): First-stage ignition delay in the negative temperature coefficient behavior: experiment and simulation. *Combust Flame*, Vol. 167, May 2016, pp. 14-23.
[20] Boot, M. D., Tian, M., Hensen, E. J. M., Sarathy, M. S. (2017): Impact of fuel molecular structure on auto-ignition behaviour – design rules for future high performance gasolines. *Progress in Energy and Combustion Science*, Vol. 60, May 2017, pp. 1-25.
[21] Mehl, M., Pitz, W. J., Westbrook S. K., Curran H. J. (2011): Kinetic modelling of gasoline surrogate components and mixtures under engine conditions. *Proceedings of the Combustion Institute*, Vol. 33, No. 1, 2011, pp. 193-200.
[22] Zhen, X., Wang, Y., Xu, S., Zhu, Y., Tao, C., Xu, T., Song, M. (2012): The engine knock analysis – an overview," *Applied Energy*, Vol. 92, April 2012, pp. 628-636.
[23] Abu-Qudais, M. (1996): Exhaust gas temperature for knock detection and control in spark ignition engine," *Energy Conversion and Management*, Vol. 37, September 1996, pp. 1383-1392.
[24] Grandin, B., Denbratt, I., Bood, J., Brackmann, C., Bengtsson, P-E., Gogan, A., Mauss, F., Sunden, B. (2002): Heat release in the end-gas prior to knock in lean, rich and stoichiometric mixtures with and without EGR. *SAE Technical Paper 2002-01-0239*, 2002.
[25] Qi, Y., Wang, Z., Wang, J., He, X. (2015): Effects of thermodynamic conditions on the end gas combustion mode associated with engine knock. *Combustin and Flame*, Vol. 162, No. 11, November 2015, pp. 4119-4128.
[26] Alger, T., Chauvet, T., Dimitrova, Z. (2008): Synergies between high EGR operation and GDI systems," *SAE Int J Engines*, Vol. 1, No. 1, April 2008, pp. 101-114.
[27] Towers, J. M., Hoekstra, R. L. (1998): Engine knock, a renewed concern in motorsports - a literature review. *SAE Technical Paper 983026*, 1998.
[28] Clenci, A. C., Descombes, G., Podevin, P., Hara, V. (2007): Some aspects concerning the combination of downsizing with turbocharging, variable compression ratio, and variable intake valve lift. *Proceedings of the Institute of Mechanical Engineering, Part D: Journal of Automobile Engineering*, Vol. 221, No. 10, October 2007, pp. 1287-1294.
[29] Kalghatgi, T. G., Babiker, H., Badra, J. (2015): A Simple Method to Predict Knock Using Toluene, N-Heptane and Iso-Octane Blends (TPRF) as gasoline surrogates. *SAE Int. J. Engines 8 (2):505-519*, 2015.
[30] ANSYS (2017): *ANSYS 18.1 Chemkin-Pro Tutorials Manual*. Ansys Inc., San Diego, 2017.
[31] ANSYS (2017): *ANSYS 18.1 Chemkin-Pro Getting Started Guide*. Ansys Inc., San Diego, 2017.
[32] Cai, L., Pitsch, H. (2015): Optimized chemical mechanism for combustion of gasoline surrogate fuels. *Combustion and Flame*, Vol 162, No. 5, May 2015, pp. 1623-1637.
[33] Curran, H., Gaffuri, P., Pitz, W., Westbrook, C. (2002): A comprehensive modelling study of iso-octane oxidation. *Combustion and Flame*, Vol. 129, No. 3, May 2002, pp. 253-280.

[34] Han, Z., Reitz, R. D. (1997): A temperature wall function formulation for variable-density turbulent flows with application to engine convective heat transfer modelling. *International Journal of Heat and Mass Transfer*, Vol. 40, No. 3, February 1997, pp. 613-625.
[35] Ciezki, H. K., Adomeit, G. (1993): Shock-tube investigation of self-ignition of n-heptane-air mixtures under engine relevant conditions. *Combustion and Flame*, Vol. 93, No. 4, June 1993, pp. 421-433.
[36] Minetti, R., Carlier, M., Ribaucour, M., Therssen, E., Sochet, L. R. (1995): A rapid compression machine investigation of oxidation and auto-ignition of n-heptane: Measurements and modelling. *Combustion and Flame*, Vol. 102, No. 3, August 1995, pp. 298-309.
[37] Yang, Li, Alfazazi, A., Mohan, B. Tingas, E. A., Badra, J., Hong, G., Sarathy, S. M. (2019): Development of a reduced four-component (toluene/n-heptane/iso-octane/ethanol) gasoline surrogate model," *Fuel*, Vol. 247, No. 1, July 2019, pp. 164-178.
[38] Sarathy, S. M., Atef, N., Alfazazi, A., Badra, J., Zhang, Y., Tzanetakis, T., *et al.* (2018): Reduced gasoline surrogate (toluene/n-heptane/iso-octane) chemical kinetic model for Compression Ignition Simulations. *SAE Technical Paper 2018-01-0191*, 2018.
[39] Mehl, M., Pitz, W. J., Westbrook, C. K., Curran, H. J. (2011): Kinetic modelling of gasoline surrogate components and mixtures under engine conditions. *Proceedings of the Combustion Institute*, Vol. 33, No. 1, 2011, pp. 193-200.
[40] Fieweger, K., Blumenthal, R., Adomeit, G. (1997): Self-ignition of SI engine model fuels: A shock tube investigation at high pressures. *Combustion and Flame*, Vol. 109, No. 4, June 1997, pp. 599-619.
[41] Cancino, L. R., Fikri, M., Oliveira, A. A. M., Schulz, C. (2009): Autoignition of gasoline surrogate mixtures at intermediate temperatures and high pressures: Experimental and numerical approaches. *Proceedings of the Combustion Institute*, Vol. 32, No. 1, 2009, pp. 501-508.